

# A *synthetic* ice core approach to estimate ion relocation in an ice field site experiencing periodical melt; a case study on Lomonosovfonna, Svalbard

C. P. Vega,<sup>1</sup> V. A. Pohjola,<sup>1</sup> E. Beaudon,<sup>2,\*</sup> B. Claremar,<sup>1</sup> W. J. J. van Pelt,<sup>1</sup> R. Pettersson,<sup>1</sup> E. Isaksson,<sup>3</sup> T. Martma,<sup>4</sup> M. Schwikowski,<sup>5</sup> and C. E. Bøggild<sup>6,§</sup>

[1]{Department of Earth Sciences, Uppsala University, Villavägen 16, SE-752 36 Uppsala, Sweden}

[2]{Arctic Centre, University of Lapland, 96101 Rovaniemi, Finland}

[3]{Norwegian Polar Institute, Fram Centre 9296 Tromsø, Norway}

[4]{Institute of Geology, Tallinn University of Technology, [19086](#) Tallinn, Estonia}

[5]{Paul Scherrer Institut, 5232 Villigen PSI, Switzerland}

[6]{The University Centre in Svalbard, UNIS, Pb. 156 9171, Longyearbyen, Norway}

[\*]{now at: Byrd Polar and Climate Research Center, 082A Scott Hall, 1090 Carmack Road, Columbus, OH 43210-1002, USA}

[§]{now at: Arctic Technology Centre, Technical University of Denmark, Kemitorvet, Bygning 204, 2800 Kgs. Lyngby, Denmark}

Correspondence to: C. P. Vega ([carmen.vega@geo.uu.se](mailto:carmen.vega@geo.uu.se))

## Abstract

Physical and chemical properties of four different ice cores (LF-97, LF-08, LF-09 and LF-11) drilled at Lomonosovfonna, Svalbard, were compared to investigate the effects of meltwater percolation on the chemical and physical stratigraphy of these records. A *synthetic* ice core approach was employed as reference record to estimate the ionic relocation and meltwater percolation length at this site during the period 2007–2010. Using this method, a *partial* ion elution sequence obtained for Lomonosovfonna was  $\text{NO}_3^- > \text{SO}_4^{2-} > \text{Mg}^{2+} > \text{Cl}^- > \text{K}^+ > \text{Na}^+$  with *nitrate* being the most mobile within the snowpack. The relocation length of most of the ions was in the order of 1 m during this period. In addition, by using both a positive degree day (PDD) and a snow-energy model approaches to estimate the percentage of melt at Lomonosovfonna, we have calculated a melt percentage (MP) of the total annual

Deleted: the  
Deleted:  $\text{SO}_4^{2-}$   
Deleted:  $\text{NO}_3^- >$   
Deleted:  $\text{NH}_4^+ >$   
Deleted:  $>$   
Deleted:  $>$   
Deleted:  $> \text{Ca}^{2+}$ ,  
Deleted: acidic ions  
Deleted: , with the exception of  $\text{SO}_4^{2-}$  showing relocation lengths  $> 2$  m

1 accumulation within the range between 48 and 70 %, for the period between 2007 and 2010  
2 which is above the MP range suggested by the ion relocation evidenced in the LF-syn core  
3 (i.e. MP = 30%). Using a firn-densification model to constrain the melt range, a MP of 30 %  
4 was found over the same period which is consistent with the results of the synthetic ice core  
5 approach, and a 45 % of melt for the last 60 years. Considering the ionic relocation lengths  
6 and annual melt percentages, we estimate that the atmospheric ionic signal remains preserved  
7 in recently drilled Lomonosovfonna ice cores at an annual or bi-annual resolution when  
8 weather conditions were similar to those during the 2007–2010 period.

9 **Key words:** ion relocation, percolation length, melt index, ice cores.

## 10 **1 Introduction**

11 Pollutants produced in low- and mid-latitudes are transported to the polar regions where they  
12 are included in the snow by different mechanisms, mainly wet and dry deposition,  
13 accumulating in glaciers and ice caps. Major ions, such as  $\text{SO}_4^{2-}$ ,  $\text{NO}_3^-$ ,  $\text{Na}^+$ , and  $\text{Cl}^-$ , are  
14 deposited in the snowpack and can be measured in ice cores, providing valuable information  
15 about their sources, chemical transformations in the atmosphere, and transport patterns to the  
16 sampling site (*Laj et al.*, 1992; *Goto-Azuma and Koerner*, 2001; *Kekonen et al.*, 2002;  
17 *Hastings et al.*, 2004; *Hastings et al.*, 2009). Nitrate ( $\text{NO}_3^-$ ), for example, has been used as a  
18 record for past atmospheric nitrogen oxides ( $\text{NO}_x = \text{NO}_2 + \text{NO}$ ) (*Kekonen et al.*, 2002;  
19 *Röthlisberger et al.*, 2002; *Hastings et al.*, 2005; *Hastings et al.*, 2009; *Vega et al.*, 2015b).  
20 However, this proxy has been difficult to develop since  $\text{NO}_3^-$  in snow has several sources and  
21 experiences post-depositional processes, such as photolysis, diffusion within the ice,  
22 evaporation as  $\text{HNO}_3$ , or relocation by meltwater (*Goto-Azuma et al.*, 1994; *Honrath et al.*,  
23 1999; *Rempel et al.*, 2002; *Röthlisberger et al.*, 2002). The latter has been an enigma to  
24 potential ice core sites since relocation and preferential elution of chemical species gives an  
25 altitudinal and latitudinal threshold for potential drilling sites. To make use of environmental  
26 data from outside the dry snow zones on glaciers in the polar areas, it is important to give  
27 better regional coverage of the atmospheric chemistry outside the large polar ice sheets. For a  
28 correct interpretation of the chemical ice core data from drilling sites where significant  
29 summer melting occurs, it is necessary to estimate the post-depositional effects of meltwater  
30 percolation on the chemical content of snow and ice.

31 It is known that most of the ice core drilling sites at Svalbard experience summer melting,  
32 which may damp the chemical signal of ionic species, making it difficult to understand the

1 transfer function between ion concentrations in the atmosphere and the snow (*Goto-Azuma et*  
2 *al.*, 1994; *Isaksson et al.*, 2001; *Moore et al.*, 2005; *Grinsted et al.*, 2006). Ions do not move  
3 uniformly when are removed from the snowpack by meltwater. Instead, they are released  
4 following a preferential elution (*Goto-Azuma et al.*, 1994; *Eichler et al.*, 2001; *Ginot et al.*,  
5 2010). The elution of ions is a consequence of sequential grain-scale processes during dry  
6 metamorphism (*Brimblecombe et al.*, 1985; *Schöndorf and Herrmann*, 1987; *Goto-Azuma et*  
7 *al.*, 1994) and also influenced by the pH of meltwater (*Goto-Azuma et al.*, 1994). *Moore and*  
8 *Grinsted* (2009) calculated the elution factors ( $e$ ) of several ions present in snow and ice from  
9 an ice core drilled at Lomonosovfonna, Svalbard during 1997 (LF-97). According to their  
10 results, the most mobile species in the snow were  $\text{Ca}^{2+}$ ,  $\text{Mg}^{2+}$ ,  $\text{SO}_4^{2-}$  and  $\text{NO}_3^-$  with  $\text{Na}^+$ ,  $\text{Cl}^-$ ,  
11  $\text{NH}_4^+$  and  $\text{K}^+$  being eluted later. The elution sequence changed slightly in ice, where  $\text{NO}_3^-$  is  
12 the most mobile specie and  $\text{Mg}^{2+}$  the latest ion to elute. *Moore and Grinsted* (2009), *Ginot et*  
13 *al.* (2010) and *Eichler et al.* (2001) results point to the ionic charge as the control factor in the  
14 elution process instead of the acidic character of the ion as reported by *Brimblecombe et al.*  
15 (1985) and *Goto-Azuma et al.* (1994).

16 The special characteristics of snow and firn properties on high altitude ice fields with  
17 heterogeneous stratigraphy as Lomonosovfonna are a consequence of the long winter season  
18 with air temperatures below the freezing point, enhanced snow drift by strong winds,  
19 relatively low annual snow accumulation and cold ground surfaces, punctuated by intermittent  
20 melt events. The interaction between the meltwater front formed during episodic melt events  
21 and the different stratigraphic horizons form preferential flow patterns and create a secondary  
22 stratigraphy if refreezing takes place within colder layers (*Colbeck*, 1991). The secondary  
23 stratigraphy produced by refreezing water will have a large influence in meltwater flow and  
24 discharge (*Bøggild*, 2000). During the intermittent melt periods, dislocation of water from  
25 more superficial layers percolates into the deeper stratigraphy routed as preferential meltwater  
26 flow and the formation of solute enriched ice layers during refreeze of the percolated water  
27 will affect the chemistry (i.e. ionic concentrations in this study) recorded in ice cores drilled at  
28 the high altitude ice fields of Svalbard.

29 One estimate to measure if snow melting and percolation have occurred in an ice core  
30 stratigraphy is to construct an ion ratio, based on the selection of a pair of ions that originate  
31 from the same source but have dissimilar elution coefficients, e.g.  $\text{Na}^+/\text{Mg}^{2+}$  and  $\text{Cl}^-/\text{K}^+$  as  
32 reported by *Iizuka et al.* (2002) and *Grinsted et al.* (2006). Using the logarithms of the

1 different ionic ratios as melt indices, denoted as  $W_{\text{NaMg}}$  or  $W_{\text{ClK}}$  depending upon the pair of  
2 ions selected, a reconstruction of the melting history of a particular ice core site can be  
3 reconstructed (*Grinsted et al.*, 2006). *Pohjola et al.* (2002) found that at Lomonosovfonna,  
4 about 25 % to 55 % of the annual accumulation over the 20<sup>th</sup> century **may melt and percolate**  
5 **into the underlying snow/firn**. The most mobile ions reported by *Pohjola et al.* (2002) were  
6  $\text{NO}_3^-$  and  $\text{SO}_4^{2-}$ , which presented ~50 % higher concentrations in ice compared with firn  
7 layers. On the other hand,  $\text{NH}_4^+$  presented an even distribution between firn and ice. A  
8 percolation mechanism was proposed to have an important role in the redistribution of this  
9 specie in the ice crystals after deposition. *Pohjola et al.* (2002) concluded that although some  
10 ions may have had a high mobility within the upper part of the LF-97 ice core (0–36 m deep)  
11 during anomalously warm summers, the signal was still identifiable, being retained within an  
12 annual or biannual resolution.

**Deleted:** suffered melt, with meltwater percolating through the snowpack during warm summers

13 The aim of this work is to study the temporal change of the snow/firn chemical and physical  
14 stratigraphy on the ice field Lomonosovfonna, Svalbard. In this study we will use data from  
15 shallow ice cores and snow pits repeatedly studied in 2008, 2009, 2010 and 2011 at  
16 Lomonosovfonna to investigate the temporal and vertical change in the stratigraphy and ion  
17 composition of the snow/firn column. To manage the sequential change in ion concentrations  
18 we will create a *synthetic* ice core using the top layer (~1 year accumulation) of different  
19 shallow ice cores and snowpits to have a reference record to assess the relocation of major  
20 ions by meltwater and the percolation length at the site during recent years. In addition, the  
21 melt percentage of the annual accumulation at Lomonosovfonna is obtained by using a  
22 positive degree day and a snow-energy model approach, and used together with the *synthetic*  
23 core to infer the effects of meltwater on the ionic signals present in recent ice cores drilled at  
24 Lomonosovfonna.

## 25 **2 Methods**

### 26 **2.1 Study sites**

27 Four ice cores (LF-97, LF-08, LF-09 and LF-11) and a 1.50 m deep snowpit (SP LF-10) were  
28 considered in this study, all retrieved at the Lomonosovfonna ice cap, which is one of the  
29 highest glaciated areas in Svalbard with an elevation of ~1250 m a.s.l. (*Isaksson et al.*, 2001;  
30 *Beaudon*, 2012; *Vega et al.*, 2015b) (**Figure 1**). Lomonosovfonna is located northeast of  
31 Longyearbyen, which is the largest settlement in Svalbard, and Pyramiden, a smaller  
32 settlement where coal mining activities were carried out until 1998. Two of the ice cores (LF-

**Deleted:** Figure 1

1 97 and LF-08) were drilled at the highest point of the ice cap ca. 100 m apart from each other,  
2 while the LF-09 and LF-11 ice cores were drilled ca. 4.5 km east-south-east from the site  
3 cored in 1997 and 2008 ([Figure 1](#), [Error! Reference source not found.](#)).

Deleted: Figure 1

Deleted: Table 1

## 4 2.2 Sampling and analyses

5 The cutting, sampling and chemical analyses of the LF-97 and LF-08 ice cores are reported by  
6 *Kekonen et al.* (2005, and references therein) and *Beaudon* (2012), respectively. The LF-09  
7 and LF-11 ice core cutting and SP LF-10 sampling were done in clean conditions, wearing  
8 clean overalls, face masks and powder free gloves. All materials employed to collect the  
9 samples were rinsed with ultra-pure water (18 M $\Omega$ ) and kept in clean plastic bags. [Ions were](#)  
10 [quantified using a Metrohm ProfIC 850 ion chromatographer;](#) samples and standards were  
11 melted and handled under laminar flow hood (class 100) to minimize any contamination from  
12 the laboratory environment. Samples and standards were placed in the auto-sampler covered  
13 with aluminium foil to avoid any dust contamination. Three sample blanks (made of ultra-  
14 pure water) were analysed at the beginning and the end of every batch. Sample checks (bulk-  
15 snow from Ny-Ålesund or Uppsala) were analysed every ten samples to ensure the  
16 replicability of the measurements within a batch. The analytical error was below 5 % for each  
17 ion. Detection limits (D.L.) for each ion were calculated as the average value of six blanks  
18 plus 1.68 times the standard deviation ( $\sigma$ ) of the six measurements (i.e.  
19  $D.L. = average_{blank} + 1.68 \times \sigma_{blank}$ ), being below 0.3  $\mu\text{eq L}^{-1}$  for all ions.

Deleted: s

20 Water stable isotopes ( $\delta^{18}\text{O-H}_2\text{O}$ ) were analysed at the Institute of Geology at Tallinn  
21 Technical University, Estonia. The measurements were done with a Picarro L2120-i water  
22 isotope analyser (cavity ringdown spectroscopy technology) with a high precision vaporizer  
23 A0211. All isotope measurements were calibrated in a two-point scale against the  
24 international standards VSMOW (Vienna Standard Mean Ocean Water) and VSLAP (Vienna  
25 *Standard Light Antarctic Precipitation*). The reproducibility of replicate analysis for  $\delta^{18}\text{O-}$   
26  $\text{H}_2\text{O}$  measurements was estimated to be  $\pm 0.1 \%$ .

27 The ice layer and grain size were inspected in each core section by visual examination on a  
28 lighted bench located in the cold laboratory ( $-20 \text{ }^\circ\text{C}$ ) at the Norwegian Polar Institute. Bulk  
29 density was calculated by weighing and measuring each ice core piece of the LF-97, LF-09  
30 and LF-11 cores. Density in the LF-08 core was estimated using high resolution dielectric  
31 profiling (DEP) with a threshold value of 900  $\text{kg m}^{-3}$ , i.e. values above that were set to NaNs.

1 The stratigraphic melt index was calculated as the percentage of clear ice present in the ice  
2 core (considering the ice core length in m w.e. (m water equivalent)).

### 3 **2.3 Synthetic ice core construction**

4 In order to estimate the effects of meltwater percolation on the chemical record at  
5 Lomonosovfonna, a *synthetic* ice core approach was implemented. This consists of building  
6 an unperturbed ice core using only the top meter of the snowpack from different ice cores (top  
7 meters of the LF-08 and LF-09 cores and the SP LF-10 snowpit), thus, constructing a snow-  
8 firm record covering the previous year until the date of the sampling/drilling of the previously  
9 sampled/drilled snowpit/core during the period 2007–2010 (**Error! Reference source not**  
10 **found.**). Consequently, summer snow has been included in the synthetic core (Table 2);  
11 therefore, no error due to exclusion of this layer is present in the time scale. However, the  
12 summer snow in the synthetic core has most probably experienced melting at each interval,  
13 i.e. in the summer of 2009, 2008 and 2007, correspondently. Since each new segment of the  
14 synthetic core starts in the spring of the corresponding year (Table 2), ions that could have  
15 been relocated from the summer layer above are not present in the new core segment due to  
16 its different origin (Table 2).

Deleted: Table 2

### 17 **2.4 Calculation of the meltwater**

18 In order to quantify the meltwater produced at Lomonosovfonna, two independent approaches  
19 were used: a simple positive degree day (PDD) model using instrumental temperature data  
20 from stations near Lomonosovfonna; and a coupled snow-energy balance model (*van Pelt et*  
21 *al.*, 2012) that delivers snowmelt as output.

#### 22 **2.4.1 PDD model**

23 We considered temperature instrumental data from three different sites in Svalbard:  
24 Longyearbyen Airport, Sveagruva and Ny-Ålesund (data from the Norwegian Meteorological  
25 Institute, <http://eklima.met.no/>). To estimate the number of positive degree days (PDD) at  
26 Lomonosovfonna, a lapse rate of  $-0.0044\text{ }^{\circ}\text{C m}^{-1}$  was used (*Pohjola et al.*, 2002). An annual  
27 average number of 37 PDD at Lomonosovfonna was calculated when using the combined  
28 temperature records of Longyearbyen Airport, Sveagruva and Ny-Ålesund (i.e. average value  
29 of daily temperatures from the three stations), during the period between 1989–2010. The  
30 meltwater production was calculated as described by *Pohjola et al.* (2002), using the melt

1 capacity of snow as a function of the PDD at Lomonosovfonna, considering the degree day  
2 factor (DDF) as 3.0 mm water °C<sup>-1</sup> d<sup>-1</sup> found at Svalbard after calibration against stake  
3 measurements (Nuth *et al.*, 2012). In a recent study by Claremar (2013) that employs Polar  
4 Weather Research and Forecast [model](#) (Polar WRF) (Skamarock *et al.*, 2008; Wilson *et al.*,  
5 2011) a value for DDF of 25 mm °C<sup>-1</sup> d<sup>-1</sup> of water was found at Lomonosovfonna. However,  
6 this DDF value has proven to be too high due to the poor modelling of the net mass balance at  
7 Lomonosovfonna when using [Polar](#) WRF temperatures and snow accumulation rates for the  
8 last decades (Claremar, 2013). [Consequently](#), to calculate the meltwater we employed the  
9 DDF value proposed by Nuth *et al.* (2012) which is more realistic for Lomonosovfonna.

Deleted: ,

Deleted: modelled temperatures,

Deleted: polar

Deleted: Consequently

## 10 2.4.2 Coupled snow-energy balance model

11 The coupled model was developed to simulate the surface energy balance and subsurface  
12 conditions, in order to predict melt, refreezing and runoff at Nordenskiöldbreen, Svalbard and  
13 it is described by van Pelt *et al.* (2012) and (2014). The meltwater refreezing output of the  
14 grid point located at 1200 m a.s.l. was used in this study to account for melting at the  
15 Lomonosovfonna ice core site. At this elevation runoff does not occur; which implies that all  
16 the available water at the surface (from melt and rain) refreezes within the snow/firn pack.

## 17 3 Results and discussion

### 18 3.1 Dating of the ice cores

19 The LF-97 ice core has been dated by different methods (e.g. radioactive horizons,  $\delta^{18}\text{O}$ -H<sub>2</sub>O  
20 cycles counting, volcanic horizons) having a time scale that covers the past 800 years  
21 (Isaksson *et al.*, 2001; Pohjola *et al.*, 2002). An updated time scale for this ice core has been  
22 recently published by Divine *et al.* (2011).

23 During the 2009 drilling campaign at Lomonosovfonna, two parallel ice cores were drilled:  
24 the LF-09 (36 m deep, this study) and a longer core LF-09<sub>deep</sub> (149.5 m deep) (Wendl *et al.*,  
25 2015). Tritium (<sup>3</sup>H) measurements done in the LF-09<sub>deep</sub> ice core estimate the 1963 <sup>3</sup>H  
26 horizon (Pinglot *et al.*, 1999) at 23.6 m w.e., with a resulting accumulation rate of  
27 0.51 m y<sup>-1</sup> w.e. between the <sup>3</sup>H radioactive horizon and the top of the ice core (Wendl *et al.*,  
28 2015). In addition, the high resolution chemical data available for the LF-09 ice core (samples  
29 taken each 8 cm) allowed the use of a multilinear regression method (MLR) developed by  
30 Moore *et al.* (2012) to account for volcanic layers in the non-sea salt sulfate concentrations. A  
31 detailed description of the usage of the MLR method on the dating of the LF-09 ice core can

1 be found in *Vega et al.* (2015b). In addition to the MLR method, an automated  $\delta^{18}\text{O}\text{-H}_2\text{O}$   
2 cycles counting routine was used in the dating. This method counted  $\delta^{18}\text{O}\text{-H}_2\text{O}$  annual cycles  
3 that had an amplitude  $A > 0.1 \text{ ‰}$  ( $\delta^{18}\text{O}$  uncertainty in the SMOW scale) and a frequency in  
4 the sub-annual cycle ( $\lambda_{\text{seas}}$ ) larger than 1/3 the accumulation rate (*Pohjola et al.*, 2002). Using  
5 both methods, the time scale for the LF-09 core was estimated to span between 1957–2009  
6 (*Vega et al.*, 2015b).

7 The LF-08 and LF-11 ice cores were dated using the automated  $\delta^{18}\text{O}\text{-H}_2\text{O}$  annual cycles  
8 counting routine and by comparing the  $\text{Cl}^-$  record with the respective LF-09 ice core profile.

9 The LF-08 core data has only been interpreted between the top and 6.4 m due to the presence  
10 of an anomalous column of clear ice between 6.4 m and 10.6 m deep which is suspected to be  
11 originated by a water-filled crevasse. Clear ice layers of this length have never been observed  
12 in any of our ice coring efforts. The summit has a few, but deeply cutting extensional  
13 crevasses not visible under the snow cover in the spring. The time scales for the cores were  
14 estimated to cover the 2000–2008 and 2004–2011 periods for the LF-08 and LF-11 (*Vega et*  
15 *al.*, 2015a) ice cores, respectively.

**Deleted:** The LF-08 core data has only been interpreted between the top and 6.4 m due to the presence of an anomalous column of clear ice between 6.4 m and 10.6 m deep which is suspected to be originated by a water-filled crevasse.

16 The time scale of the SP LF-10 snowpit was obtained by assuming a constant snow  
17 accumulation rate over the depth-scale, resulting in time coverage between 2009.4–2010.4.

**Deleted:** 1989

### 18 3.2 Major ions

19 All the ionic concentrations were binned to annual averages to obtain equally spaced time  
20 series of one year resolution, which can be compared in between the different ice cores.  
21 Having all the chemical species as annual averages, their concentrations ( $c_i$ ) were normalized  
22 to the mean value for each specie in each ice core record, during the total overlapping period  
23 (1957–2009) to compare the variations of the ions in the different ice cores (Equation 1).

$$24 \quad c_N = \frac{c_i - c_{\text{mean}}}{\sigma}, \quad \text{Equation 1}$$

25 where  $c_N$  is the normalized concentration of a given ion,  $c_{\text{mean}}$  is the ion mean in the specific  
26 ice core or strata, and  $\sigma$  is the standard deviation of the series.

27 When comparing the annual average concentrations between the different ice cores, some of  
28 the peaks show a lag between the different records which likely is associated with the  
29 uncertainty of the dating of the three different ice cores. We applied a 5-year moving average



smoothing to the annual chemical data (Figure 2). The dating error of the LF-08 and LF-09, in respect to the LF-97 ice core, was estimated as  $\pm 2$  years. We found that similar temporal variations experienced by the different ions were registered in the different Lomonosovfonna ice cores during the overlapping period studied (Figure 2).

Deleted: Figure 2

Error! Reference source not found, shows the Pearson coefficient (R), and the Wilcoxon rank sum test between the different species in the LF-97 and LF-09 ice cores, smoothed out with 5-year moving averages of the annual data. The Wilcoxon rank sum test was also applied to the ion series in the LF-08 and LF-09 cores to evaluate the hypothesis that ion concentrations in the different LF-cores are samples from continuous distributions with equal medians. The R-values between the LF-08 and LF-09 cores were not calculated since the overlapping period using 5-year moving average was too short. The R-values and the results of the Wilcoxon test in Error! Reference source not found, suggest that the LF-97 and LF-09 cores, and the LF-08 and LF-09 cores have comparable chemical records for all ions during the period 1956–1996 and 2000–2008, respectively. Consequently, they can be used to interpret the main chemical and climatic patterns at Lomonosovfonna at this resolution.

Deleted: Figure 2

Deleted: Table 3

Deleted: R-values

Deleted: and the LF-09 and LF-09 ice cores

Deleted: LF-97 and LF-08

Deleted: ice

Deleted: Table 3

Deleted: ice

Deleted: . However, the correlation coefficients measured in the LF-08 and LF-09 ice cores are not significant at the 95 % confidence interval (with the exception of  $Mg^{2+}$ ,  $R = -0.53$ ).

### 3.3 Ionic distribution in the snowpack

In order to investigate to what degree ions are eluted from the snowpack when meltwater percolates, we first compared the log-transformed concentrations ( $\text{Log}(c)$ ) of the different species measured in the LF-09 and LF-11 ice cores at different snowpack facies: i.e. snow, ice, and firn. The chemical record of the LF-09 ice core was considered only during the period 2004–2009 when it overlaps with the LF-11 ice core.

Figure 3 shows that the median  $\text{Log}(c)$  of ions in the LF-09 ice core is significantly higher, at a 95% confidence level, in the snow compared to ice and firn for  $SO_4^{2-}$ ,  $Cl^-$ ,  $NO_3^-$ ,  $Br^-$ ,  $Na^+$  and  $K^+$ , with higher  $\text{Log}(c)$  values also for  $Ca^{2+}$  and  $Mg^{2+}$ , however, not significant. Moreover, concentrations show similar medians in firn and ice. On the other hand, Figure 4 shows that median  $\text{Log}(c)$  in the LF-11 ice core are significantly higher in the snow compared to both ice and firn only for  $Br^-$  and  $Mg^{2+}$ , with  $SO_4^{2-}$  median in snow being only significantly higher than in ice. The rest of the ions present even concentrations in all the strata, with the exception of  $NH_4^+$  which shows a higher median concentration in ice compared to firn and snow.

Deleted: Figure 3

Deleted:

Deleted: all species.

Deleted: means

Deleted: Figure 4

Deleted: ion concentrations

Deleted: most of the ions, with the exception of  $NO_3^-$  and  $NH_4^+$ ,  $NO_3^-$

Deleted: s

Deleted: while

Deleted: show

Deleted: s

Deleted: mean

1 Previous work by *Pohjola et al.* (2002) focused on the effect of periodic melting in the  
2 chemical record of an ice core drilled at Lomonosovfonna (LF-97) shows that the average  
3 ionic concentrations of the different ionic species were higher in the ice facies than in the firn  
4 layers. We observed ~~that this is only significant for  $\text{NH}_4^+$  in the LF-11 ice core. Since all ions~~  
5 in the LF-09 and LF-11 ice cores within the period 2004–2011 (10 m deep) are mostly  
6 distributed between the snow and firn, we infer that ions in this section of the ice cores have  
7 not been heavily relocated by meltwater percolation. Since the amount of meltwater  
8 production at the summit of Lomonosovfonna is unknown for the studied years, three  
9 different approaches were used in order to estimate and relate it to ionic snowpack  
10 redistribution (see section 3.5.).

Deleted:  $\text{Br}^-$  and

Deleted: measured in the LF-09 ice core  
and  $\text{F}^-$  and  $\text{NH}_4^+$  measured

11 In order to elucidate the evolution of meltwater production over time, the chemical melt index  
12 ( $W_{\text{NaMg}}$ ), defined as  $\text{Log}(\text{Na}^+)/(\text{Mg}^{2+})$  (using ionic concentrations in  $\mu\text{eq L}^{-1}$ ) (*Iizuka et al.*,  
13 2002; *Grinsted et al.*, 2006) was calculated in the different Lomonosovfonna ice cores ([Figure](#)  
14 [5](#)). This chemical approach is based on the selection of a pair of ions that have the same  
15 source but dissimilar elution coefficients within the snowpack, e.g.  $\text{Na}^+/\text{Mg}^{2+}$  and  $\text{Cl}^-/\text{K}^+$   
16 (*Grinsted et al.*, 2006). Positive  $W_{\text{NaMg}}$  values indicate that melting has most probably  
17 occurred. This is the case of the four Lomonosovfonna ice cores ([Figure 5](#)) which show  
18 positive melt indices during the last 60 years. As observed in [Figure 5](#), melting at the drilling  
19 site is far from being constant; a period of particular high melt is evident during mid-1980s to  
20 mid-1990s which is concomitant with a period of relatively high number of PDDs at  
21 Lomonosovfonna. Although the above mentioned method is useful to infer melting regimes at  
22 Lomonosovfonna at large time scales (i.e. decadal to centennial), it is not suitable to infer  
23 melting at sub-, and multi-annual resolutions; therefore, the *synthetic* ice core approach  
24 described in this study presents a suitable option.

Deleted: Figure 5

Deleted: Figure 5

Deleted: Figure 5

### 25 3.4 Synthetic ice core

26 Assuming that snowmelt does not occur during winter, and considering that precipitation  
27 records of different Svalbard sites show that most of the precipitation is registered during the  
28 winter and autumn seasons (*Førland et al.*, 2011), it is expected that the synthetic ice core  
29 (LF-syn) captures the unperturbed chemistry of the ~~winter, autumn, summer~~ and early spring  
30 seasons between spring 2007–2010. [Figure 6](#) shows the annual precipitation cycle at  
31 Longyearbyen airport and Ny-Ålesund stations and the precipitation amount and snow

Deleted: n-winter

Deleted: Figure 6

1 accumulation from the two stations and the LF-syn core during the period 2007–2011. The  
2 snow accumulation in the LF-syn core was calculated as the length (in m w.e.) between two  
3 LF-syn core samples which in average represent 1.2 months of accumulation. Both, the  
4 meteorological and the ice core records are coherent with each other, depicting higher  
5 accumulation rates during the autumn/winter period than spring/summer. Consequently, it is  
6 expected that the LF-syn ice core is representative of the snow accumulation regime at  
7 Lomonosovfonna during 2007–2010. The flat accumulation observable during the winter  
8 2010 is due to the assumption of a linear time scale when dating each snow layer of the  
9 snowpit dug out in 2010 (SP LF-10). In addition, the average annual mass loading of each ion  
10 was calculated for the period 1980–2009 by averaging the annual ion loads calculated in the  
11 LF-97 and LF-09 cores. This procedure averaged out the possible effects of percolation and  
12 relocation of ions between the strata corresponding to different years. This estimate was then  
13 compared with the mass loading of the different ions corresponding to individual years in the  
14 LF-syn core (i.e. 2007–2010) which are assumed to represent cumulative autumn-winter-early  
15 spring snow accumulation unaltered by meltwater percolation or ion relocation. It was found  
16 that the 5-year LF-syn record represents between 70–200 % of the 30-year average ion mass  
17 loading with  $\text{NH}_4^+$  and  $\text{Mg}^{2+}$  located at the bottom and top percentage boundaries,  
18 respectively, and  $\text{NO}_3^-$  and  $\text{SO}_4^{2-}$  representing 94 % and 111 % of the average, respectively.  
19 Keeping in mind that the mass loading for most of the ions show increasing values since 2005  
20 (not shown), thus, influencing the percentage of average mass loading in the LF-syn core, we  
21 consider that this synthetic core is adequate to investigate ion relocation during the period  
22 2007–2011. The LF-syn core was then compared with the LF-11 core to evaluate the effects  
23 of ion elution/deposition between 2007–2010 (recorded in the LF-11 ice core) compared to  
24 the unperturbed LF-syn ice core (Figure 7). Since the top part of the LF-11 core (0–0.6 m  
25 w.e.) was not used to construct the LF-syn core (Table 2), and to avoid any bias caused for the  
26 snow accumulated after the spring 2010 and 2011, this period was not considered in the  
27 normalization of the LF-11 ionic concentrations. Figure 7, shows that the LF-11 record has  
28 noticeable large  $c_N$  peaks, e.g. around summer 2009, that can be associated with the increase  
29 in ionic concentrations by the relocation of ions by the refreezing of percolation water. Figure  
30 8, shows the differences between  $c_N$  in both ice cores (LF-11 – LF-syn) calculated after  
31 interpolating the records at 0.01-year time steps to homogenize the data. A lowpass filter  
32 (half-year moving average) was used to filter out high frequency processes superimposed to  
33 the percolation and relocation effect (Figure 8); consequently, a cutting threshold of half a

Deleted:

Deleted: Figure 7

Deleted: To

Deleted: Figure 7

Deleted: Figure 8

Deleted: -

1 year was assumed for the relocation of ions. Using the filtered time series shown in Figure 8,  
 2 we considered a relocation period when the differences in  $c_N$  are positive. Positive differences  
 3 indicate higher ionic concentrations in the LF-11 ice core with respect to the LF-syn ice core,  
 4 therefore, ice-firn layers enhanced in ions due to relocation by percolation water. Negative  
 5 differences indicate ionic elution happening at that layer. Consequently, the study period was  
 6 divided in four sub-periods denoted with roman numbers (Figure 8). It is worth saying, that  
 7 even though the LF-11 core was used for comparison with the LF-syn core only between  
 8 2007.4–2010.4, the effects of melt water produced and percolated during the summer of 2010  
 9 are recorded in the LF-11 core. Consequently, Period I encompasses the melting season of the  
 10 summer-spring months of 2010 (elution period). Period II reflects the deposition period after  
 11 the spring-summer of 2010. Period III represents elution occurred between summer of 2009  
 12 and summer of 2008; and Period IV encompasses a deposition period from spring of 2008 to  
 13 spring of 2007. From Figure 8, it can be observed that most of ions (with the exception of  
 14  $\text{NH}_4^+$  and  $\text{Ca}^{2+}$ ) share similar elution/deposition features in Periods I–IV. We estimate a  
 15 minimum ionic relocation length as the difference in depth between the minimum/maximum  
 16 (elution/deposition)  $c_N$  peaks observed in Periods I–II (Figure 8, Table 4). The difference was  
 17 not calculated in Periods III–IV since the time series are truncated before reaching a  
 18 maximum value, however the elution minima are noted in Table 4. The relocation length was  
 19 calculated for all ions, with the exception of  $\text{NH}_4^+$  and  $\text{Ca}^{2+}$ .  
 20 Considering the elution/deposition  $c_N$  peaks estimated above, a partial ionic elution scheme at  
 21 Lomonosovfonna for the period 2007–2010 can be inferred, resulting in  $\text{NO}_3^-$  being the most  
 22 mobile ion. This partial elution scheme agrees with previous studies done at Lomonosovfonna  
 23 (Moore and Grinsted, 2009) which found that  $\text{NO}_3^-$  was highly mobile. The partial elution  
 24 sequence and ion relocation lengths shown in Table 4, suggest that the ions are relocated by  
 25 meltwater at short lengths, probably trapped in thin and medium-thick ice layers present  
 26 within the ice column observable in the LF-97, LF-09 and LF-11 cores (Figure 9), or in  
 27 refrozen water that soaks the firn column filling the pore space. Nevertheless, the results  
 28 shown in Figure 8 and Table 4 are not absolute for the full length of the Lomonosovfonna  
 29 core but rather the case for years with apparently moderate melting (e.g.  $\text{MP} < 50\%$ ). In years  
 30 were summers are warmer and/or longer, ions may percolate further down in the snowpack  
 31 and get trapped in medium-thick to thick ice layers which start to form at about 3–10 m deep  
 32 in the ice column as observable in the LF-97 and LF-09 cores (Figure 9).

**Deleted:** We considered a relocation peak when the differences in  $c_N$  are higher than twice the standard deviation of the normalized concentrations of each ion (dashed red line in

**Deleted:** Figure 8

**Deleted:** such as  $\text{Cl}^-$ ,  $\text{Na}^+$

**Deleted:** and  $\text{NO}_3^-$  present clear deposition/elution  $c_N$  peaks. On the other hand,  $\text{SO}_4^{2-}$  only shows a deposition peak with an elution zone, rather than a single elution peak. This can be interpreted as  $\text{SO}_4^{2-}$  eluting steadily and further down the snowpack than the other ions during this period (Figure 8Figure 8).<sup>1</sup>

**Deleted:** maximum/minimum (deposition/elution)

**Deleted:** , as shown in Figure 8 and presented in Table 4. T

**Deleted:**  $\text{SO}_4^{2-}$

**Deleted:** which does not show an elution peak that is significant within the time window studied

**Deleted:** For the ions that show more than one significant deposition/elution peak, the relocation length calculated considering the second maximum/minimum  $c_N$  peak is also shown in Table 4.¶

**Deleted:** deposition

**Deleted:** elution

**Deleted:** the

**Deleted:** last 5 years

**Deleted:** s

**Deleted:**  $\text{SO}_4^{2-}$  being the most mobile ion and

**Deleted:** the least mobile one

**Deleted:** .

**Deleted:** differs

**Deleted:** mainly in

**Deleted:** locating

**Deleted:** at the end of the

**Deleted:** elution sequence

**Deleted:** However, it should be noticed that we estimated two possible relocation lengths based in the depth difference between deposition/elution peaks (as explained before). Therefore, considering a  $\text{NO}_3^-$  relocation length of 1.16 m, the elution sequence agrees with previous findings by Moore and Grinsted (2009), locating the acidic ions ( $\text{SO}_4^{2-}$  and  $\text{NO}_3^-$ ) as more mobile than the others ions.

**Deleted:** less mobile

**Deleted:** the

**Deleted:** More mobile

1 In order to estimate how the ionic relocation length during 2007–2010 is connected to  
2 meltwater percolation length and snowpack melting, we have estimated the melt percentage at  
3 Lomonosovfonna using two different methods, as shown in the following section.

### 4 **3.5 Meltwater production at Lomonosovfonna**

5 The produced meltwater obtained by using the PDD and snow-energy model approaches are  
6 shown in Figure 10 for the period 1979–2012 (calculated using PDD and instrumental  
7 temperatures), and 1989–2010 (using the snow-energy model). The production of meltwater  
8 at the summit of Lomonosovfonna has increased at a rate of  $+0.0011 \text{ m y}^{-1}$  w.e toward the last  
9 decades (corresponding to the linear trend of meltwater production calculated with the PDD  
10 and instrumental temperatures approach, Figure 10). The average melting between 1989–2010  
11 was calculated as 0.17 m w.e. when using the PDD and instrumental temperature approach.  
12 When considering the period between 2007–2010 (Figure 11), the melting shows alternating  
13 warm and cold years (2007/2009, and 2008/2010, respectively), with meltwater average  
14 values of 0.19 m w.e. and 0.27 m w.e. when using the instrumental temperatures, and the  
15 coupled snow-energy model, respectively. Alternatively, meltwater production was also  
16 calculated by using modelled temperatures obtained with the Polar WRF model at the summit  
17 of Lomonosovfonna and a DDF of  $3.0 \text{ mm water } ^\circ\text{C d}^{-1}$ . An average meltwater production of  
18 0.07 m w.e. and 0.05 m w.e. were obtained for the periods 1989–2010 and 2007–2010,  
19 respectively when using the Polar WRF modelled temperatures. The meltwater production  
20 obtained by the Polar WRF approach gives values that are significantly lower than the  
21 meltwater obtained by using both the PDD and snow-energy model approaches which is a  
22 consequence of the less number of PDDs per year estimated at the summit of  
23 Lomonosovfonna when using the Polar WRF model (i.e. 18 PDDs per year between 1989–  
24 2010) explained by the fact that the Polar WRF model produces lower surface temperatures  
25 compared to the lapse-rate based temperatures at this site. Therefore, the meltwater calculated  
26 by using Polar WRF modelled temperatures were not considered in this study.

**Deleted:** The meltwater production shows a minimum around 1995, which is present when using both approaches (Figure 10).

27 In order to estimate the impact of melting on the snowpack ionic content at the summit of  
28 Lomonosovfonna, the percentages of the annual snow accumulation that melts (Table 5) were  
29 calculated using the results in Figure 10 and Figure 11 and the annual accumulation rate  
30 between 2007–2010 at Lomonosovfonna obtained from the LF-09 and LF-11 cores. The melt  
31 percentage (MP) obtained by using the instrumental temperatures (48% for the period 2007–  
32 2010) was in the order of previously reported values of 47 % of melt during the warmest

1 years and 28 % during the coldest, during the period 1976–1995 (*Pohjola et al.*, 2002). The  
2 relatively high MP values obtained in this study for the period 2007–2010 can be explained  
3 by the increase in temperatures at the site with a consequent steady increase of the number of  
4 PDD at the summit of Lomonosovfonna at a rate of  $0.4 \text{ d y}^{-1}$  for the period 1979–2012 in  
5 which instrumental temperatures exist in all the three stations used, Sveagruva, Ny-Ålesund  
6 and Longyearbyen airport; the MPs calculated using the PDD approach over the period 1979–  
7 2010 show a steady increase of  $1 \text{ \% y}^{-1}$  in line with the trend in decreasing the annual snow  
8 accumulation in  $-0.01 \text{ m y}^{-1}$  w.e. during the same period (accumulation data from the LF-09  
9 ice core).

10 However, the calculated MPs using the PDD approach and the snow-energy do not agree with  
11 the results obtained by the synthetic core approach which suggest that melting during the  
12 2007–2010 period has not been high (i.e. < 50 %) which is also supported by the stratigraphy  
13 observed in the LF-09 and LF-11 cores (Figure 9).

Deleted: moderate

14 Due to the dissimilar results of MP obtained using the PDD and snow-energy model  
15 approaches (Table 5), we compared the density profiles of the shallow ice cores used in this  
16 study (LF-08, LF-09 and LF-11) with the total layer density values obtained using a simple  
17 firm-densification model (*Reeh et al.*, 2005). The ice core density profiles were binned in  
18 annual averages in order to be comparable with the output of the firm-densification model. As  
19 described by *Reeh et al.* (2005), the model requires both annual average temperatures and  
20 snow accumulation at the study site as input, which were set as  $-18.3 \text{ °C}$  and  $0.39 \text{ m w.e.}$ ,  
21 according to instrumental temperatures from Sveagruva, Svalbard Airport and Ny-Ålesund  
22 (the lapse rate employed to calculate the temperatures at the Lomonosovfonna summit was  
23  $-0.0044 \text{ °C m}^{-1}$ ), and average accumulation rates obtained from the LF-09 and LF-11 ice  
24 cores, respectively, for the period between 2007–2010. The firm-densification model also  
25 requires the surface snow density, which was set as  $350 \text{ kg m}^{-3}$ , and a defined spatial  
26 resolution, set as  $0.5 \text{ m}$ . The firm-densification model considers the percentage of melting as  
27 one of the input variables, showing output density values versus depth. Output densities of  
28  $900 \text{ kg m}^{-3}$  are expected when the percentage of melt reaches 100 %. Four different melt  
29 scenarios were considered: MP equal to a) 20 %, b) 30 %, c) 45 %, and d) 70 %. The results  
30 of the comparison between the real ice core density profiles and the output of the firm-  
31 densification model are shown in Figure 12.

1 According to Figure 12, the firn-densification model shows better agreement with the  
2 measured density profiles in the top 10 m when the MP was set between 20 % and 30 %. This  
3 agrees with the physical melt index of the LF-09 ice core (22 %), calculated as the percentage  
4 of clear ice present in the ice core (considering the ice core length in m w.e.). However, the  
5 agreement between the firn-densification model and the density profiles is poor for depths  
6 deeper than 10 m (Figure 12 a–b) considering this range of MP. Figure 12 c–d, show the  
7 comparison between the firn-densification model and the density profiles using a MP of 45 %  
8 and 70 %. The agreement between the model and the measurements is better through the  
9 whole depth profile when setting the MP to 45 % (Figure 12 c). This agrees with the physical  
10 melt index of the LF-97 ice core (50 %), calculated between 1957 and 1997, however, it is not  
11 consistent with the physical melt index of the LF-09 ice core (25 %), calculated for the same  
12 period.

13 Considering the results shown in Table 5 and the firn-densification model output shown in  
14 Figure 12 a–d, it is plausible to think that the MP at Lomonosovfonna is not straight forward  
15 to estimate either using a simple PDD or the snow-energy model approach. Moreover, the use  
16 of Polar WRF temperatures at Lomonosovfonna as input to obtain the MP at the site is ruled  
17 out since it predicts MP values considerably lower than the values suggested by the density  
18 profiles both measured and modelled (i.e. an average MP of 12 % for the period 2007–2010  
19 when Polar WRF modelled temperatures and a DDF of 3.0 mm water °C d<sup>-1</sup> are used to  
20 calculate the meltwater production). It also needs to be considered that the firn-densification  
21 model assumes a constant melt index during the ice core time span. Therefore, the firn-  
22 densification model does not include the variability in meltwater production at  
23 Lomonosovfonna through time which is key to the understanding of ion relocation within the  
24 snowpack at long time scales; however, the MP estimated here are suitable to understand the  
25 ionic relocation and water percolation during the period 2007–2010.

26 Figure 13 shows a comparison between the LF-11 and the LF-syn ice core depth–time scale.  
27 It is clear from Figure 13 that the depth differences between the ice cores (black and grey  
28 lines) can be related to a partial melting of the snowpack and refreezing of the meltwater  
29 taking place between the 2007–2011 period, as evidenced by the ionic relocation. An estimate  
30 of the decrease in depth of the LF-syn ice core by the effects of snowpack melting considering  
31 a MP = 20, 30, 48 and 70 % during 2007–2010 as suggested by the firn-densification model,  
32 MPs obtained using the PDD approach (using instrumental temperatures) and the snow-

1 energy model is shown in Figure 13. It can be observed that a MP = 20–30 % results in a LF-  
2 syn ice core depth-time scale highly similar to the depth-time scale of the LF-11 ice core  
3 during the 2007–2010 period, confirming that the MP during that period is coherent with the  
4 results of the firn-densification model but not with the PDD results shown in table Table 5.  
5 This relatively low MP reinforces the hypothesis that during this period, ion relocation took  
6 place at shallow depths (0.5–2 m) and that the meltwater percolation depth was most probably  
7 in the same order, with refreezing of meltwater within the snowpack pore space or by forming  
8 thin ice layers (0.03–0.15 m) (Figure 9).

Deleted: at  
Deleted: moderate  
Deleted: (

#### 9 4 Conclusions

10 By comparing different ice cores from Lomonosovfonna and using a *synthetic* ice core  
11 approach, we have been able to estimate the elution signal and relocation length of different  
12 ions measured at the study site, in order to assess the transfer function between the  
13 atmospheric ionic concentrations and the concentration in snow and ice.

14 Our results show good agreement between the ionic records of three different ice cores drilled  
15 during different years, using normalized concentrations and five year moving averages.  
16 Therefore, we reiterate that the different ice core records from Lomonosovfonna all share the  
17 same climatic and chemical features, despite the fact that cores have been retrieved in  
18 different years, were sampled at different resolutions, and were analysed at different  
19 laboratories. Our conclusion is that summer melting does not degrade the climatic signals.

Deleted: analyzed

20 By using the *synthetic* ice core approach, we could estimate a partial elution sequence for the  
21 summit of Lomonosovfonna, as NO<sub>3</sub><sup>-</sup> > SO<sub>4</sub><sup>2-</sup>, Mg<sup>2+</sup>, Cl<sup>-</sup>, K<sup>+</sup>, Na<sup>+</sup>, which agrees with  
22 previous reports. This elution sequence points towards the acidic ions as being the most  
23 mobile within the Lomonosovfonna snowpack. Considering the differences between the LF-  
24 11 and the LF-syn ice cores, we conclude that the relocation length of most the ions during  
25 the 2009–2010 period is in the order of 1 m, therefore, the ions are eluted and re-deposited  
26 within the annual snow layer, considering present average accumulation rate at  
27 Lomonosovfonna (i.e. < 1 m of snow per year). Consequently, using 5-year moving averages  
28 of the ionic data allows having comparable records when different ice cores are used

Deleted: n  
Deleted: SO<sub>4</sub><sup>2-</sup> >  
Deleted: NH<sub>4</sub><sup>+</sup> >  
Deleted: >  
Deleted: >  
Deleted: >  
Deleted: Ca<sup>2+</sup>,  
Deleted: 2007

29 By using the PDD and the snow-energy model approaches to estimate the percentage of melt  
30 (MP) at Lomonosovfonna, we have estimated average annual MP in the range of 48% to 70%  
31 for the period between 2007–2010, in contrast to the lesser melting suggested by the LF-syn

Deleted: According to our results, only SO<sub>4</sub><sup>2-</sup> shows percolation lengths that could potentially reach deeper than the previous year of snow accumulation (>2 m), which affects the annual atmospheric signal and prevents any high resolution (seasonal, annual) analysis to be possible in Lomonosovfonna ice cores. However, as we have concluded before  
Deleted: moderate



1 core for the same period. In order to constrain the MP, we have compared different density  
2 profiles obtained at the Lomonosovfonna drilling sites with a simple firn-densification model,  
3 obtaining a most probable average annual MP of 30 % for the 2007–2010 period which is  
4 consistent with the results of the synthetic ice core approach, and 45 % of melt for the last 60  
5 years. The lower melting percentages inferred for the 2007–2010 period compared with the  
6 whole period covered by the LF.-09 core are most probably a result of a combination of  
7 relatively high snow accumulation rates and reduced PDD during the 2007–2010 period  
8 despite of the warmer conditions registered during the last decades.

9 Considering our findings, we conclude that despite of the warmer conditions and higher  
10 number of PDD registered at Lomonosovfonna during the last decades, the ionic signal  
11 affected by melting is retained within the same year of deposition for all major ions.

**Deleted:** , with the exception of  $\text{SO}_4^{2-}$   
which can possibly be re-deposited in  
previous annual layers.

## 12 **Acknowledgements**

13 The authors want to thank the Lomonosovfonna 1997, 2008 and 2009 drilling teams and NPI  
14 field logistics for their support, C. Zdanowicz and G. Engström, Uppsala University, J.  
15 Moore, Arctic Centre, J. Zábory, Stockholm University, and S. Bejai, SLU for their comments  
16 and sharing of analytical lab facilities. This work was supported within the Marie Curie Initial  
17 Training Network NSINK ITN-2007.1.1, ENV., 215503 with complementary economic  
18 support by Ymer-80, the Arctic Fieldwork Grant by the Svalbard Science Forum, Uppsala  
19 Geographical Association, Sweden, and to the EU Regional Development Foundation, project  
20 3.2.0801.12-0044.

21

22

23

## 1 **References**

- 2 Beaudon, E. 2012. Glaciochemical evidence of spatial and temporal environmental variability  
3 across Svalbard. Arctic Centre Reports 58. Lapland University Press: Rovaniemi. ISBN 978-  
4 952-484-562-5. ISSN 1235-0583.
- 5 Brimblecombe, P., Tranter, M., Abrahams, P. W., Blackwood, I., Davies, T. D., and Vincent,  
6 C. E. 1985. Relocation and preferential elution of acidic solute through the snowpack of a  
7 small, remote, high-altitude Scottish catchment. *Ann. Glaciol.*, 7, 141–147.
- 8 Bøggild, C. E. 2000. Preferential flow and melt water retention in cold snow packs in West-  
9 Greenland. *Nordic Hydrology*, 31(4/5), 287–300.
- 10 Claremar, B. 2013. Relation between meso-scale climate and glacier/snow mass balance on  
11 Svalbard, Dept. Earth Sciences, Uppsala University, SVALI Technical report. [http://ncoe-](http://ncoe-svali.org/xpdf/svali_report_d2-3-11_fin.pdf)  
12 [svali.org/xpdf/svali\\_report\\_d2-3-11\\_fin.pdf](http://ncoe-svali.org/xpdf/svali_report_d2-3-11_fin.pdf).
- 13 Claremar, B., Obleitner, F., Reijmer, C., Pohjola, V., Waxegård, A. et al. (2012). Applying a  
14 Mesoscale Atmospheric Model to Svalbard Glaciers. *Adv. Meteorol.* 321649.
- 15 Colbeck, S. C. 1991. The layered character of snow covers. *Rev. Geophys.*, 29 (1), 81–96.
- 16 Dee, D. P., Uppala, S. M., Simmons, A. J., Berrisford, P., Poli, P., et al. (2011). The ERA-  
17 Interim reanalysis: configuration and performance of the data assimilation system. *Q.J.R.*  
18 *Meteorol. Soc.*, 137: 553–597. doi:10.1002/qj.828.
- 19 Divine, D., Isaksson, E., Martma, T., Meijer, H. A. J., Moore, J., Pohjola, V., van de Wal, R.  
20 S.W., and Godtlielsen, F. 2011. Thousand years of winter surface air temperature variations  
21 in Svalbard and northern Norway reconstructed from ice-core data. *Polar Res.*, 30, 7379,  
22 doi:10.3402/polar.v30i0.7379.
- 23 Eichler, A., Schwikowski, M., and Gäggeler, H. W. 2001. Meltwater-induced relocation of  
24 chemical species in alpine firn. *Tellus*, 53B, 192–203.
- 25 Førland, E. J., Benestad, R., Hanssen-Bauer, I., Haugen, J. E., and Skaugen, T. E. (2011),  
26 Temperature and precipitation development at Svalbard 1900–2100. *Adv. Meteorol.*, 893790,  
27 doi:10.1155/2011/893790.

1 Ginot, P., Schotterer, U., Stichler, W., Godoi, M. A., Francou, B., and Schwikowski, M. 2010.  
2 Influence of the Tungurahue eruption on the ice core records of Chimborazo, Ecuador. *The*  
3 *Cryosphere*, 4, 561–568, doi:10.5194/tc-4-561-2010.

4 Goto-Azuma, K., Koerner, R. M. 2001. Ice core studies of anthropogenic sulfate and nitrate  
5 trends in the Arctic. *J. Geophys. Res.*, 106(D5), 4959–4969.

6 Goto-Azuma, K., Nakawo, M., Jiankang, H., Watanabe, O., Azuma, N. 1994. Melt-induced  
7 relocation of ions in glaciers and in a seasonal snowpack. *Snow and Ice covers: Interactions*  
8 *with the Atmosphere and Ecosystems (Proceedings of Yokohama Symposia J2, July 1993)*,  
9 IAHS Publ. no. 223, 287–297.

10 Grinsted, A., Moore, J., Pohjola, V., Martma, T., and Isaksson, E. 2006. Svalbard summer  
11 melting, continentality, and sea ice extent from the Lomonosovfonna ice core. *J. Geophys.*  
12 *Res.*, 111(D07110), doi: 10.1029/2005JD006494.

13 Hastings, M. G., Jarvis, J. C., Steig, E. J. 2009. Anthropogenic impacts on nitrogen isotopes  
14 of ice-core nitrate. *Science*, 324, 1288.

15 Hastings, M. G., Sigman, D. M., Steig, E. J. 2005. Glacial/interglacial changes in the isotopes  
16 of nitrate from the Greenland Ice Sheet Project 2 (GISP2) ice core. *Glob. Biochem. Cycles*,  
17 19, GB4024.

18 Hastings, M. G., Steig, E. J., Sigman, D. M. 2004. Seasonal variations in N and O isotopes of  
19 nitrate in snow at Summit, Greenland: Implications for the study of nitrate in snow and ice  
20 cores. *J. Geophys. Res.*, 109 (D20306), doi: 10.1029/2004JD004991.

21 Honrath, R. E., Peterson, M. C., Guo, S., Dibb, J. E., Shepson, P. B., and Campbell, B. 1999.  
22 Evidence of NO<sub>x</sub> production within or upon Ice particles in the Greenland snowpack.  
23 *Geophys. Res. Lett.*, 26, 695–698.

24 Iizuka, Y., Igarashi, M., Kamiyama, K., Motoyama, H., Watanabe, O. 2002. Ratios of  
25 Mg<sup>2+</sup>/Na<sup>+</sup> in snowpack and ice core at Austfonna ice cap, Svalbard, as an indicator of  
26 seasonal melting. *J. Glaciol.*, 48(162), 452–460.

27 Isaksson, E., Pohjola, V., Jauhiainen, T., Moore, J., Pinglot, J. F., Vaikmäe, R., van de Wal,  
28 R. S. W., Hagen, J. O., Ivask, J., Karlöf, L., Martma, T., Meijer, H. A. J., Mulvaney, R.,  
29 Thomassen, M., van den Broeke, M. 2001. A new ice-core record from Lomonosovfonna,

1 Svalbard: viewing the 1920–97 data in relation to present climate and environmental  
2 conditions. *J. Glaciol.*, 47(157), 335–345.

3 Kekonen, T., Moore, J. C., Mulvaney, R., Isaksson, E., Pohjola, V., Van De Wal, R. S. W.  
4 2002. A 800 year record of nitrate from the Lomonosovfonna ice core, Svalbard. *Ann.*  
5 *Glaciol.*, 35, 261–265.

6 Kekonen, T., Moore, J., Perämäki, P., Mulvaney, R., Isaksson, E., Pohjola, V., and van de  
7 Wal, R. S. W. 2005. The 800 year long ion record from the Lomonosovfonna (Svalbard) ice  
8 core. *J. Geophys. Res.*, 110, D07304, doi: 10.1029/2004JD005223.

9 Laj, P., Palais, J.M., Sigurdsson, H. 1992. Changing sources of impurities to the Greenland  
10 Ice-sheet over the last 250 years. *Atmos. Environ.* 26, 2627–2640.

11 Moore, J. C., Beaudon, E., Kang, S., Divine, D., Isaksson, E., Pohjola, V. A., and van de Wal,  
12 R. S. W. 2012. Statistical extraction of volcanic sulphate from nonpolar ice cores. *J. Geophys.*  
13 *Res.*, 117, D03306; DOI 10.1029/2011JD016592.

14 Moore, J. C., and A. Grinsted. 2009. Ion fractionation and percolation in ice cores with  
15 seasonal melting, *Physics of Ice Core Records II*, Supplement Issue of *Low Temperature*  
16 *Science*, 68.

17 Moore, J. C., Grinsted, A., Kekonen, T., and Pohjola, V. 2005. Separation of melting and  
18 environmental signals in an ice core with seasonal melt. *Geophys. Res. Lett.*, 32, L10501, doi:  
19 10.1029/2005GL023039.

20 Morrison, H., J. A. Curry, and Khvorostyanov, V. I. 2005, A new double-moment  
21 microphysics parameterization for application in cloud and climate models. Part I:  
22 Description. *J. Atm. Sci.*, vol. 62, no. 6, 1665–1677.

23 Nakanishi, M. and Niino H. 2006. An Improved Mellor–Yamada Level-3 Model: Its  
24 Numerical Stability and Application to a Regional Prediction of Advection Fog, *Boundary-*  
25 *Layer Meteorol.*, vol. 119, no. 2, 397–407.

26 Norwegian Meteorological Institute <http://eklima.met.no/>. Last visited: 2015-07-31.

27 Nuth, C., Vikhamar, Schuler, T. V., Kohler, J., Altena, B., and Hagen, J. O. 2012. Estimating  
28 the long-term claving flux of Kronebreen, Svalbard, from geodetic elevation changes and  
29 mass-balance modelling, *J. Glaciol.*, 58(207), 119–133.

1 Pinglot, J. F., Pourchet, M., Lefauconnier, B., Hagen, J. O., Isaksson, E., Vaikmäe, R., and  
2 Kamiyama, K. 1999. Accumulation in Svalbard glaciers deduced from ice cores with nuclear  
3 tests and Chernobyl reference layers. *Polar Res.*, 18(2), 315–321.

4 Pohjola, V. A., Moore, J. C., Isaksson, E., Jauhiainen, T., van de Wal, R. S. W., Martma, T.,  
5 Meijer, H. A. J., and Vaikmäe, R. 2002. Effect of periodic melting on geochemical and  
6 isotopic signals in an ice core from Lomonosovfonna, Svalbard. *J. Geophys. Res.*, 107(D4),  
7 4036, 10.1029/2000JD000149.

8 Reeh, N., Fisher, D. A., Koerner, R. M., and Clausen, H. B. 2005. An empirical firn-  
9 densification model comprising ice lenses. *Ann. Glaciol.*, 42, 101–106.

10 Rempel, A. W., Wettlaufer, J. S., Waddington, E. D. 2002. Anomalous diffusion of multiple  
11 impurity species: Predicted implications for the ice core climate records. *J. Geophys. Res.*,  
12 107(B12), doi:10.1029/2002JB001857.

13 Röthlisberger, R., Hutterli, M. A., Wolff, E. W., Mulvaney, R., Fischer, H., Bigler, M., Goto-  
14 Azuma, K., Hansson, M., Ruth, U., Siggaard, M-L., Steffensen, J. P. 2002. Nitrate in  
15 Greenland and Antarctic Ice cores: a detailed description of post-depositional processes. *Ann.*  
16 *Glaciol.*, 35, 209–216.

17 Schöndorf, T., and Herrmann, R. 1987. Transport and chemodynamics of organic  
18 micropollutants and ions during snowmelt. *Nordic Hydrology*, 18, 259–278.

19 Skamarock, W. C., Klemp, J. B., Dudhia, J., Gill, D. O., Barker, D. M., Duda, M. G., Huang,  
20 X.-Y., Wang, W., and Powers, J. G. 2008. A description of the advanced research WRF  
21 version 3. NCAR/TN-475+STR, NCAR Technical Notes, Mesoscale and Microscale  
22 Meteorology Division, National Center for Atmospheric Research, Boulder, Colorado, USA.

23 Van Pelt, W. J. J., Oerlemans, C. H. Reijmer, V. A. Pohjola, R. Pettersson, and J. H. Van  
24 Angelen. 2012. Simulating melt, runoff and refreezing on Nordenskiöldbreen, Svalbard, using  
25 a coupled snow and energy balance model. *The Cryosphere*, 6, 641–659, doi: 10.5194/tc-6-  
26 641-2012.

27 Van Pelt, W. J. J., Pettersson, R., Pohjola, V. A., Marchenko, S., Claremar, B., and  
28 Oerlemans, J. 2014. Inverse estimation of snow accumulation along a radar transect on  
29 Nordenskiöldbreen, Svalbard. *J. Geophys. Res. Earth Surf.*, 119, 816–835,  
30 doi:10.1002/2013JF003040.

- 1 Vega, C. P., Björkman, M. P., Pohjola, V. A., Isaksson, E., Pettersson, R., Martma, T., Marca,  
2 A. D, Kaiser, J. 2015a. Nitrate stable isotopes and major ions in snow and ice samples from  
3 four Svalbard sites. *Polar Res.*, 34, 23246, <http://dx.doi.org/10.3402/polar.v34.23246>.
- 4 Vega, C. P., Pohjola, V. A., Samyn, D., Pettersson, R., Isaksson, E., Björkman, M. P.,  
5 Martma, T., Marca, A. D, Kaiser, J. 2015b. First Ice Core Records of Nitrate Stable Isotopes  
6 from Lomonosovfonna, Svalbard. *J. Geophys. Res. Atmos.*, 120, doi:10.1002/2013JD020930.
- 7 Wendl, I. A., Eichler, A., Isaksson, E., Martma, T., and Schwikowski, M. 2015. 800 year ice-  
8 core record of nitrogen deposition in Svalbard linked to ocean productivity and biogenic  
9 emissions. *Atmos. Chem. Phys.*, 15, 7287–7300, doi:10.5194/acp-15-7287-2015.
- 10 Wilson, A. B., D. H. Bromwich, K. M. Hines. 2011. Evaluation of Polar WRF forecasts on  
11 the Arctic System Reanalysis domain: Surface and upper air analysis. *J. Geophys. Res.*, 116,  
12 D11112, doi: 10.1029/2010JD015013.
- 13

1 **Tables**

2 Table 1 Drilling site and ice core description for the three different cores used in this study.

<u>Ice core</u>	<u>Drilling date</u>	<u>Location</u>	<u>Elevation (m a.s.l.)</u>	<u>Length (m)</u>	<u>Reference</u>
<u>LF-97</u>	<u>May 1997</u>	<u>78° 51' N 17° 25' E</u>	<u>1250</u>	<u>121.6</u>	<u>Isaksson et al. (2001)</u>
<u>LF-08</u>	<u>Mar. 2008</u>	<u>78° 51' N 17° 24' E</u>	<u>1250</u>	<u>10.6</u>	<u>Beaudon (2012)</u>
<u>LF-09</u>	<u>Mar. 2009</u>	<u>78° 49' N 17° 25' E</u>	<u>1200</u>	<u>36.0</u>	<u>Vega et al. (2015b)</u>
<u>SP LF-10</u>	<u>Mar. 2010</u>	<u>78° 49' N 17° 25' E</u>	<u>1200</u>	<u>1.5</u>	<u>This work</u>
<u>LF-11</u>	<u>Apr. 2011</u>	<u>78° 49' N 17° 25' E</u>	<u>1200</u>	<u>7.6</u>	<u>Vega et al. (2015a)</u>

3

1 | Table 2 Synthetic ice core construction using the different Lomonosovfonna shallow cores  
 2 | (LF-08 and LF-09) and SP LF-10 snowpit. \*The top meter of the LF-11 was not used to  
 3 | construct the synthetic ice core but it is shown here as reference to account for the final depth  
 4 | of the synthetic core.

<u>Ice core</u>	<u>Depth interval</u> <u>(m w.e.)</u>	<u>Time interval</u> <u>(year)</u>
<u>LF-11*</u>	<u>0.0–0.6</u>	<u>2011.4–2010.4</u>
<u>SP LF-10</u>	<u>0.6–1.4</u>	<u>2010.4–2009.3</u>
<u>LF-09</u>	<u>1.4–1.8</u>	<u>2009.3–2008.3</u>
<u>LF-08</u>	<u>1.8–2.3</u>	<u>2008.3–2007.4</u>



1 Table 3 Top table: Pearson coefficients (*R*) and Wilcoxon rank sum test results (*p*-values), at a  
 2 95 % confidence interval, between the different ions measured in the LF-97 and LF-09 ice  
 3 cores (normalized concentrations and smoothed out as 5-year running averages). The  
 4 overlapping period is 1957–1996 (top table). *p*-values of the Pearson correlation have been  
 5 corrected for the reduced degrees of freedom introduced by the 5-year smoothing. Significant  
 6 values (correlation,  $p < 0.05$ ; Wilcoxon rank sum test  $p > 0.05$ ) are shown in italics. Bottom  
 7 Table: Wilcoxon rank sum test at a 95 % confidence interval between the different ions  
 8 measured in the LF-08 and LF-09 ice cores (normalized concentrations and smoothed out as  
 9 5-year running averages). The overlapping period is 2000–2008. *N* represents the sample size,

- Deleted: at a 95 % confidence interval
- Deleted: t-test
- Deleted: .
- Deleted:
- Deleted: (top table)
- Deleted: t-test
- Deleted: and in the LF-08 and LF-09 ice cores (bottom table) (normalized concentrations and smoothed out as 5-year running averages).
- Deleted: Significant values ( $p < 0.05$ ) are shown in italics. The overlapping period is 1957–1997 (top table) and 1989–2008 (bottom table).
- Deleted: t-test
- Deleted: 0.13
- Deleted: 0.01
- Deleted: 0.13
- Deleted: 0.04
- Deleted: 0.01
- Deleted: 0.39
- Deleted: 0.46
- Deleted: 0.06
- Deleted:
- Deleted: *R*
- Deleted: -0.21
- Deleted: 0.02
- Deleted: 0
- Deleted: -0.30
- Deleted: 0.32
- Deleted: -0.16
- Deleted: -0.23
- Deleted: -0.53

*LF-97 and LF-09 ice cores*

<i>Ion</i>	<i>Cl<sup>-</sup></i>	<i>NO<sub>3</sub><sup>-</sup></i>	<i>SO<sub>4</sub><sup>2-</sup></i>	<i>Na<sup>+</sup></i>	<i>NH<sub>4</sub><sup>+</sup></i>	<i>K<sup>+</sup></i>	<i>Ca<sup>2+</sup></i>	<i>Mg<sup>2+</sup></i>
<i>R</i> ( <i>N</i> =36)	0.46	0.64	0.56	0.49	0.77	0.66	0.36	0.72
<i>Wilcoxon rank sum test</i> ( <i>p</i> -value, <i>N</i> =36)	0.32	0.13	0.35	0.16	0.15	0.61	1.00	0.34

*LF-08 and LF-09 ice cores*

<i>Wilcoxon rank sum test</i> ( <i>p</i> -value) ( <i>N</i> =5)	0.84	0.10	0.22	0.55	0.02	0.69	1.00	0.10
---	------	------	------	------	------	------	------	------

10

1 | Table 4 Minimum relocation length estimated for each ion measured in the LF-11 ice core.

<i>Ion</i>	<i>SO<sub>4</sub><sup>2-</sup></i>	<i>Mg<sup>2+</sup></i>	<i>Cl<sup>-</sup></i>	<i>K<sup>+</sup></i>	<i>Na<sup>+</sup></i>	<i>NO<sub>3</sub><sup>-</sup></i>
<i>Periods I-II: Relocation length (m)</i>	<u>1</u>	<u>1</u>	<u>1</u>	<u>1</u>	<u>1</u>	<u>1.2</u>
<i>Deposition maximum (year)</i>	<u>2009.76</u>	<u>2009.76</u>	<u>2009.76</u>	<u>2009.76</u>	<u>2009.76</u>	<u>2009.61</u>
<i>Periods III-IV Elution minimum (year)</i>	<u>2008.18</u>	<u>2008.66</u>	<u>2008.76</u>	<u>2008.76</u>	<u>2008.76</u>	<u>2008.18</u>

- Deleted: R
- Deleted: Secondary relocation peaks are also depicted.
- Deleted: >2.05
- Deleted: 1.09
- Deleted: 0.89
- Deleted: 0.89
- Deleted: 0.79
- Deleted: 0.66
- Deleted: Peak
- Deleted: 2009.5
- Deleted: 2008.6–2009.5
- Deleted: 2008.8–2009.5
- Deleted: 2007.8–2009.5
- Deleted: 2008.8–2009.5
- Deleted: 2008.9–2009.5
- Deleted: Secondary peak (m) ...

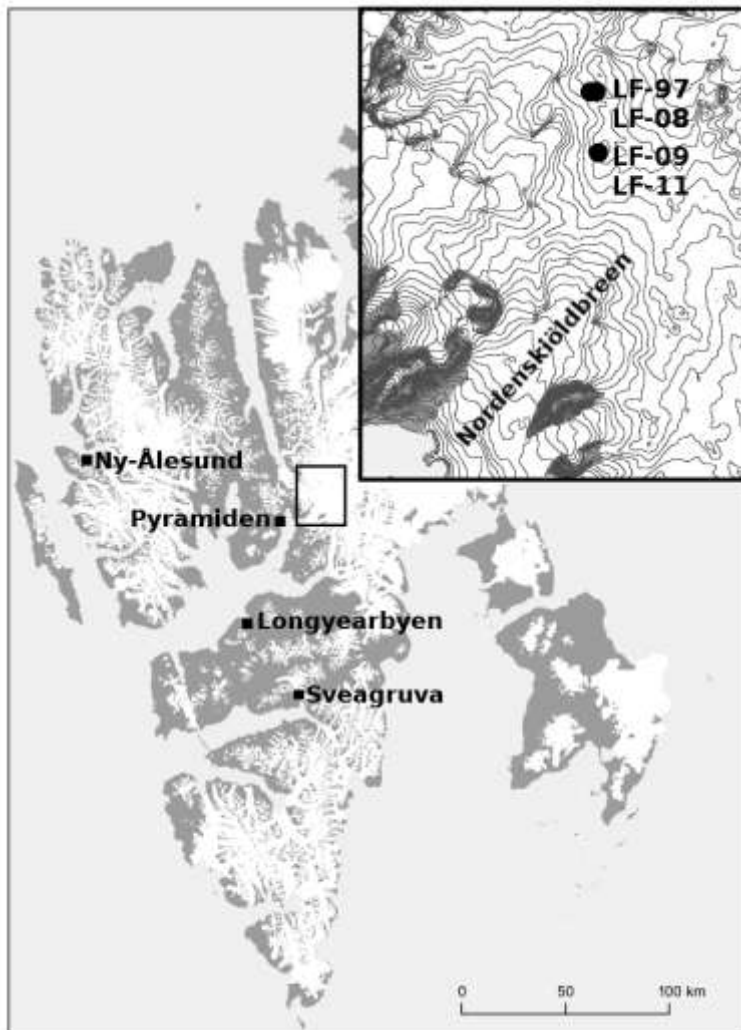
2

1 Table 5 Percentages of melted annual snow accumulation (MP) calculated with the PDD  
2 approach (Pohjola et al., 2002; Nuth et al., 2012) using instrumental temperatures, and the  
3 snow-energy model (van Pelt et al., 2012).

<u>Year</u>	<u>MP (%)</u>	
	<u>Instrumental</u> <u>temperatures</u>	<u>Snow-energy</u> <u>model</u>
<u>2010</u>	<u>34</u>	<u>52</u>
<u>2009</u>	<u>55</u>	<u>81</u>
<u>2008</u>	<u>34</u>	<u>68</u>
<u>2007</u>	<u>69</u>	<u>78</u>
<u><b>Average</b></u>	<u><b>48</b></u>	<u><b>70</b></u>

4

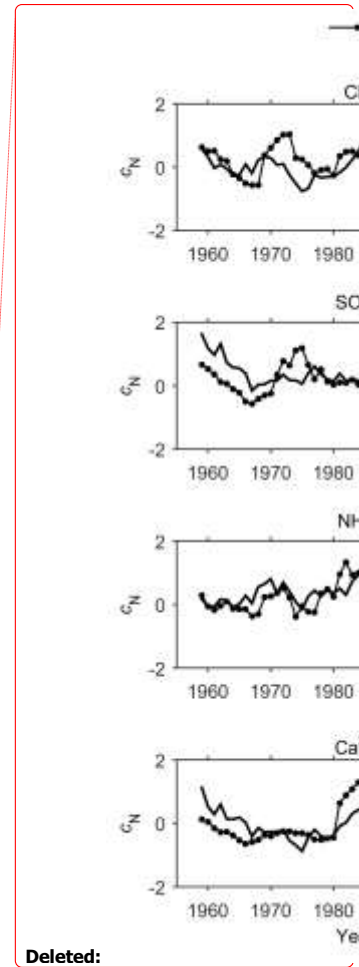
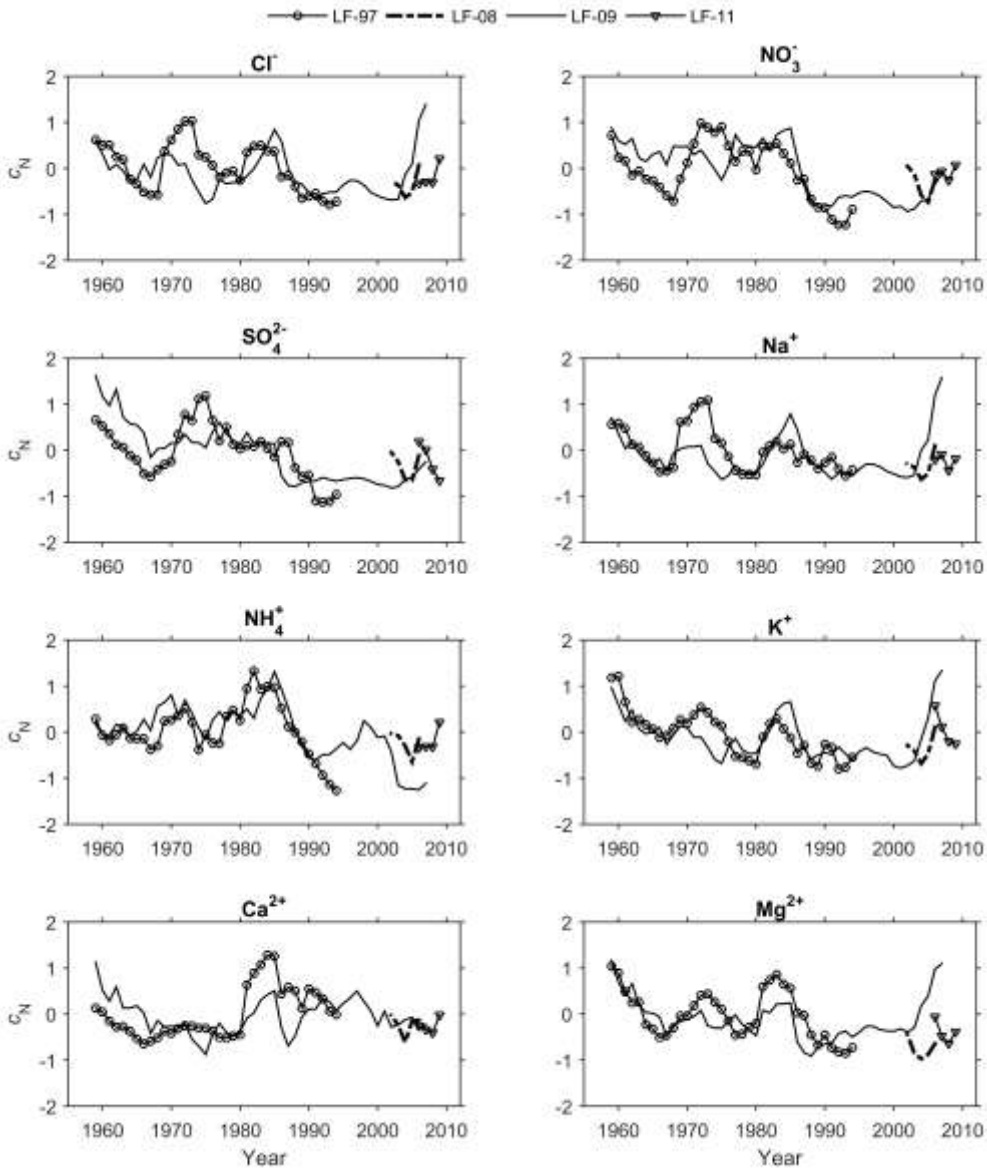
1 **Figures**



2

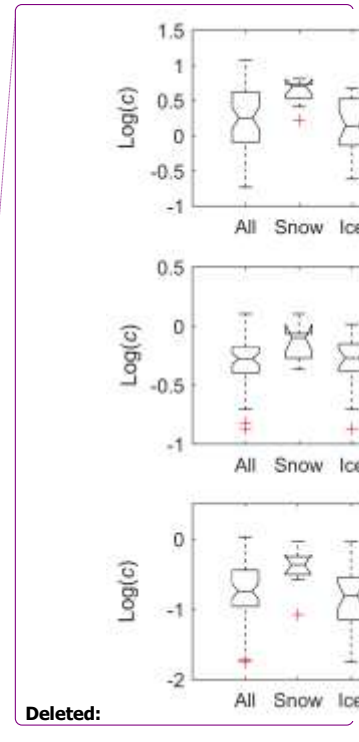
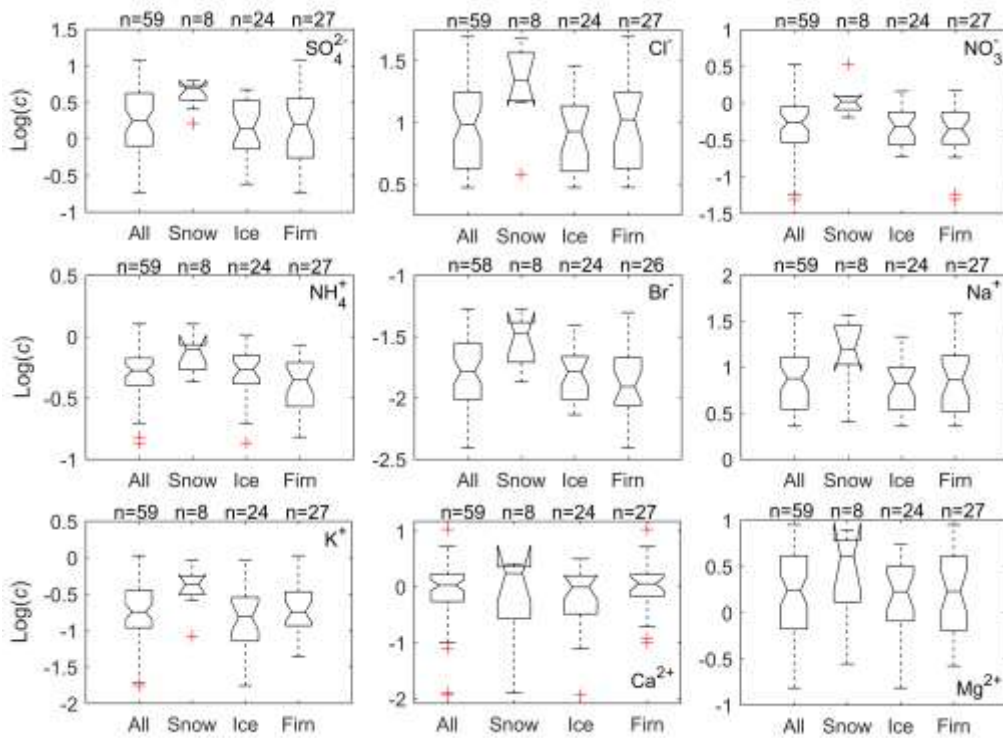
3 | Figure 1. Map of Svalbard showing the main settlements: Longyearbyen, Ny-Ålesund and  
4 | Pyramiden, and the LF-97, LF-08, LF-09 and LF-11 drilling sites at Lomonosovfonna.

Deleted: 1



Deleted:

1  
 2 Figure 2 Comparison of normalized ionic concentrations ( $c_N$ ) in the different LF-ice cores  
 3 using a 5-year moving average.  
 4

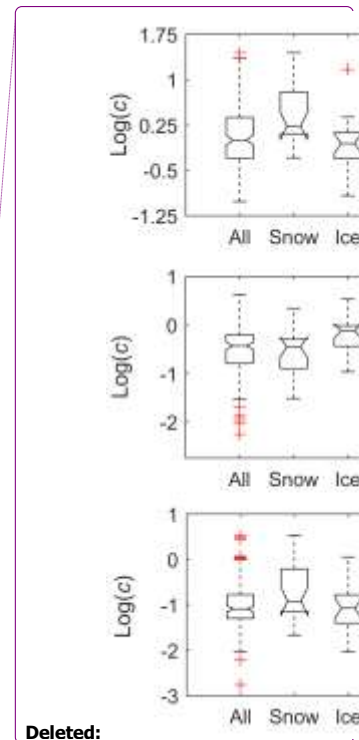
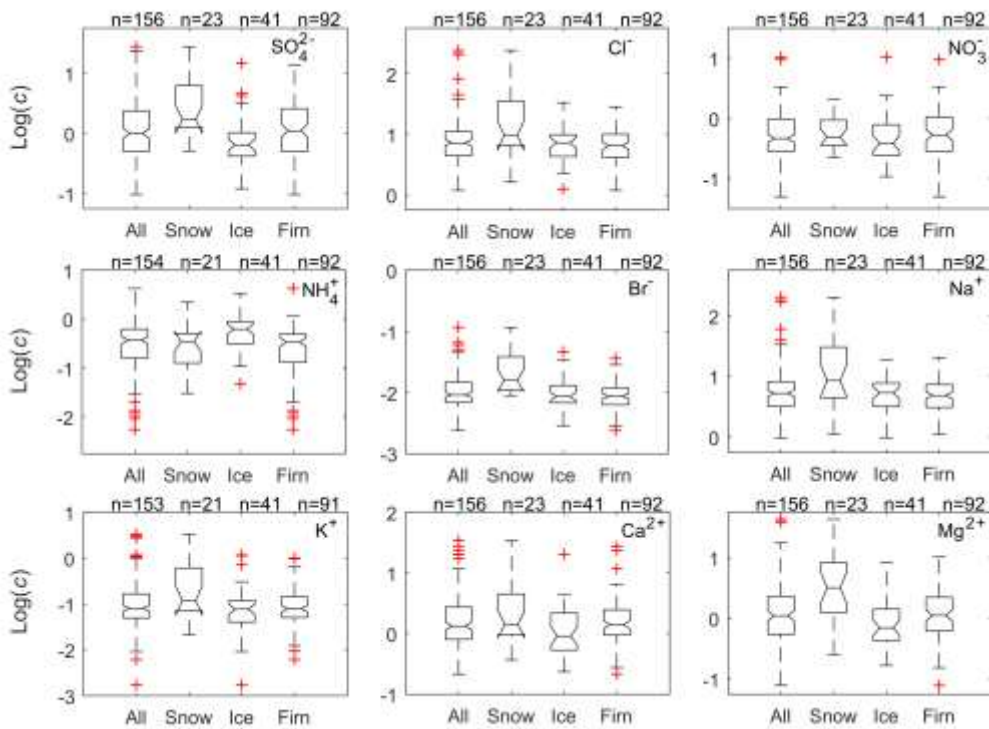


Deleted: 3

Deleted: 3

1  
 2 Figure 3 Box plot of log-transformed ionic concentrations (Log(c)) found in the different  
 3 stratigraphic units in the LF-09 ice core between 2004 and 2009. n represents the sample size  
 4 in each stratigraphic unit, and whiskers are Tukey style.

5

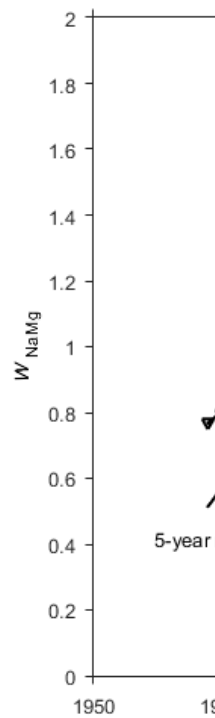
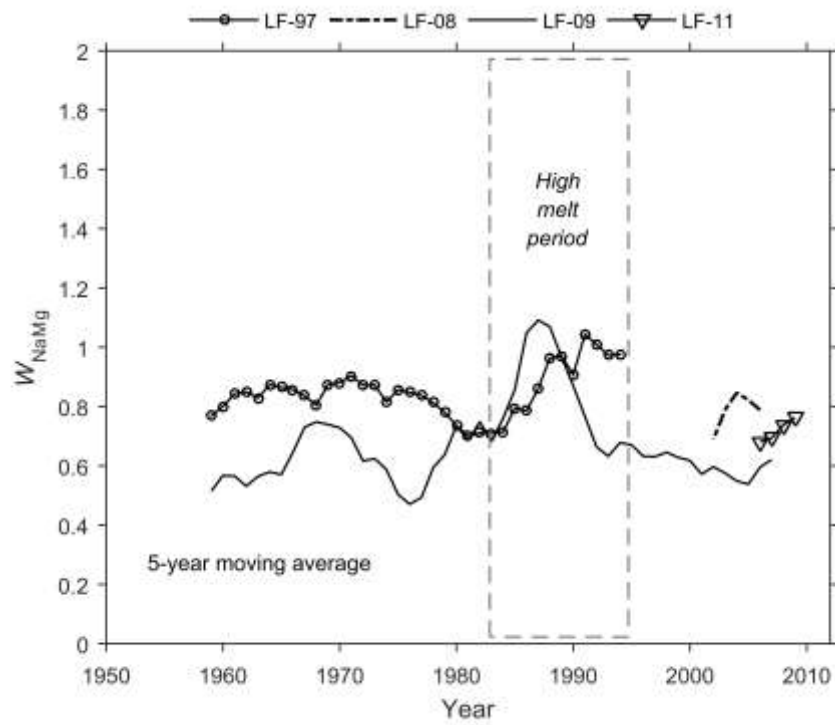


Deleted:

Deleted: 4

1  
2 Figure 4 Box plot of ionic concentrations ( $\text{Log}(c)$ ) found in the different stratigraphic units in  
3 the LF-11 ice core between 2004 and 2011.  $n$  represents the sample size in each stratigraphic  
4 unit, and whiskers are Tukey style.

5

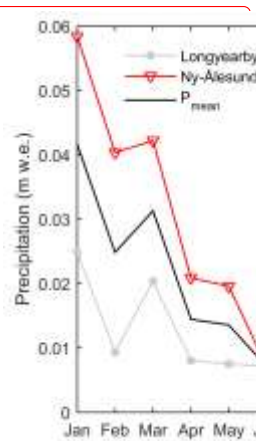
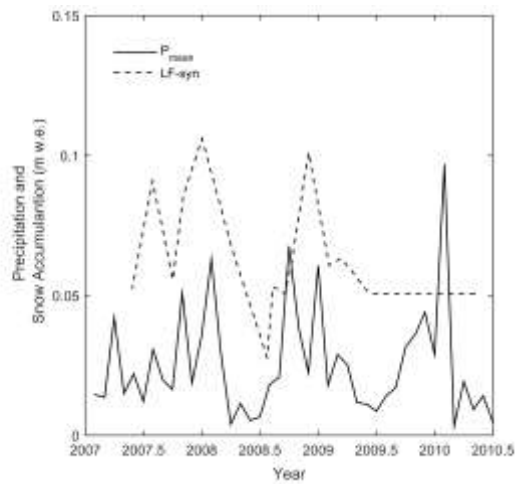
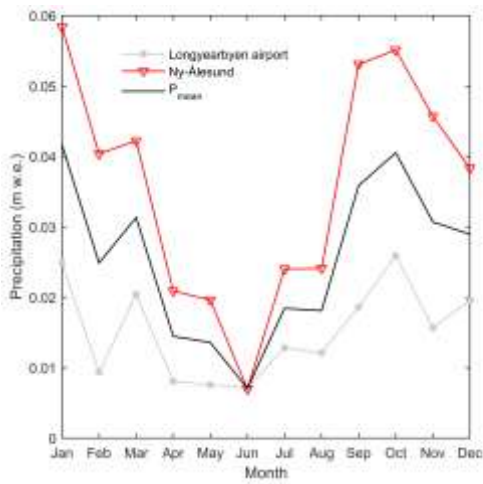


1  
2  
3  
4  
5

Figure 5. Melt index  $W_{NaMg}$  calculated in the different Lomonosovfonna ice cores. The values correspond to 5-year moving averages. The dashed lines indicates a high melting period during mid-80s to mid-90s.

Deleted:  
Deleted: 5  
Deleted: rectangle



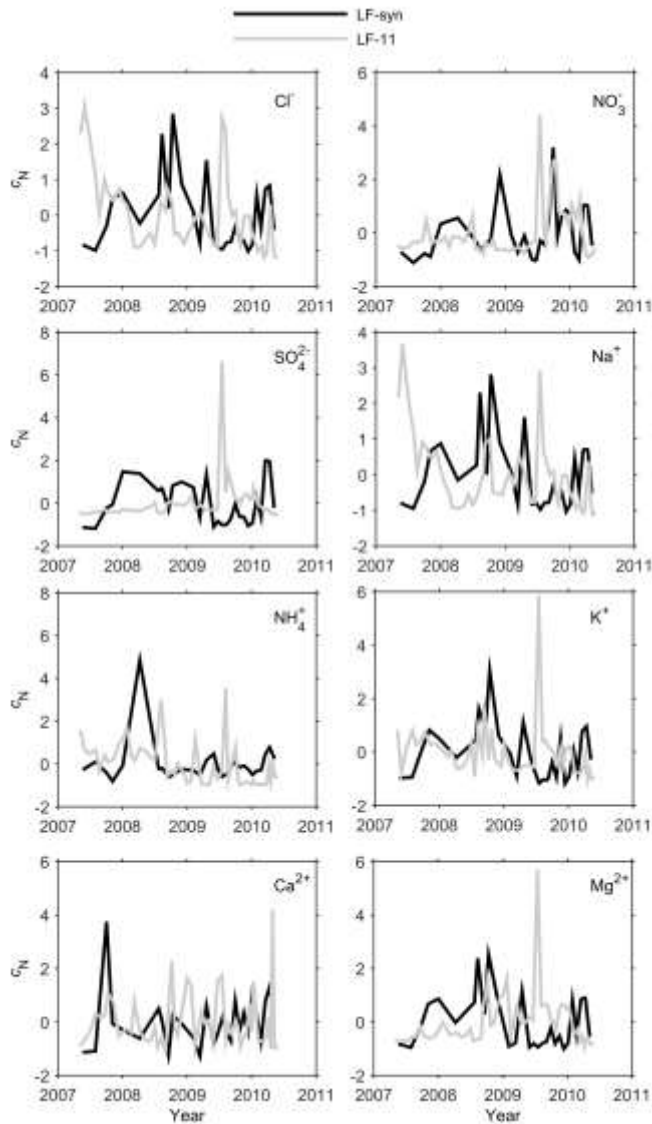


Deleted:

Deleted: 6

1  
 2 Figure 6 Annual precipitation cycle at Longyearbyen airport and Ny-Ålesund for the period  
 3 2007–2011 (left) and monthly precipitation amount at the stations and snow accumulation at  
 4 Lomonosovfonna given by the LF-syn core (right).

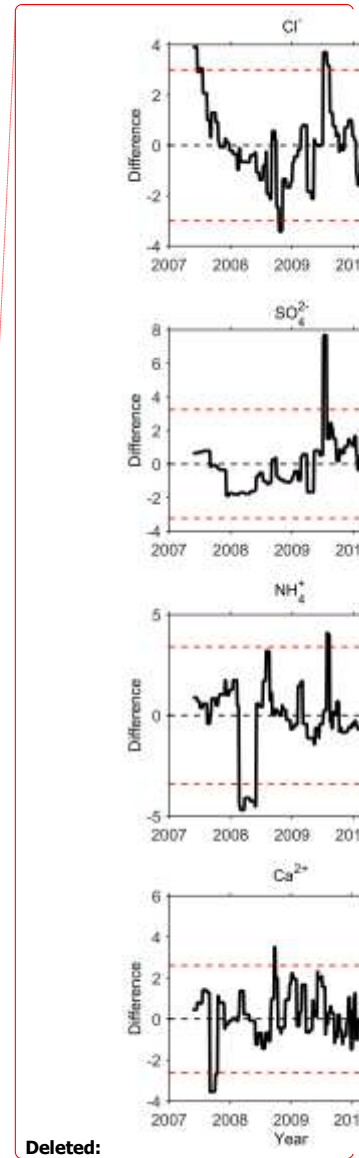
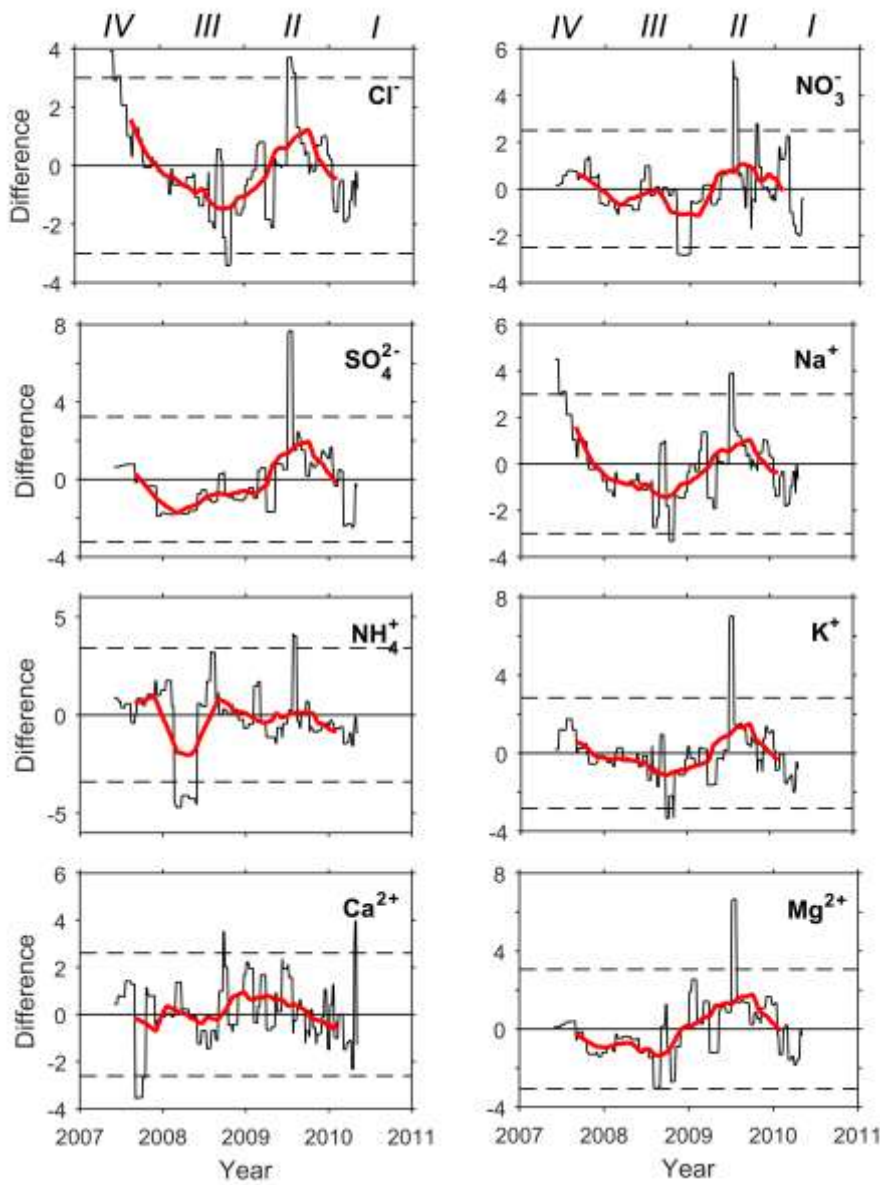
5  
 6



1  
 2 | Figure 7 Comparison between a *synthetic* ice core (LF-syn, black) and the LF-11 ice core  
 3 | (grey). Ionic concentrations are normalized ( $c_N$ ) to mean values according to the LF-syn ice  
 4 | core time scale.

Deleted: 7

5



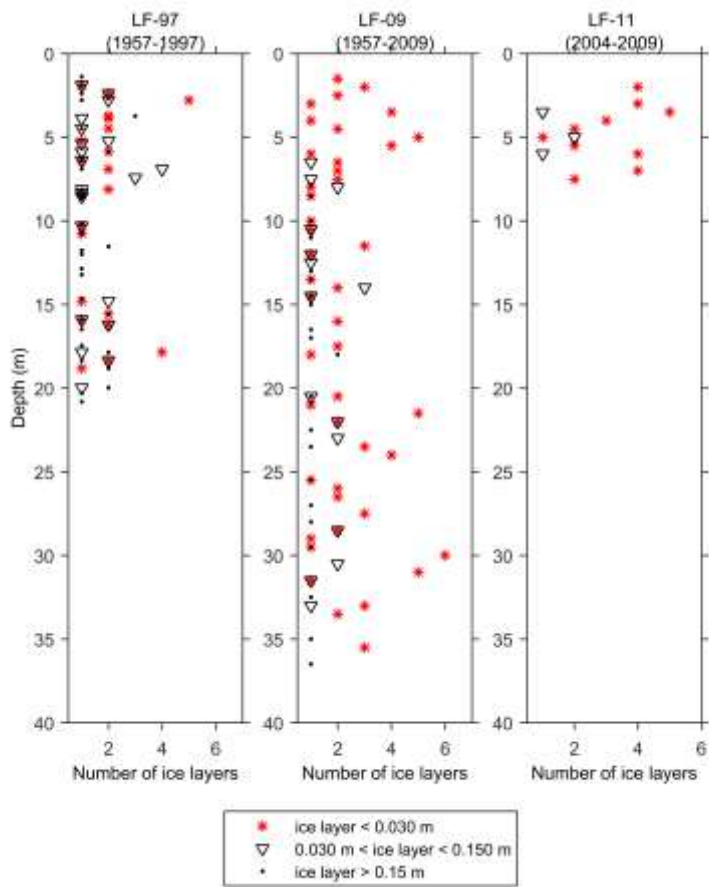
Deleted:

1  
 2 Figure 8. Difference between the normalized ionic concentrations ( $c_N$ ) in the LF-11 and the  
 3 LF-syn ice cores (black line). Twice the standard deviation (dashed red line) and zero values  
 4 (horizontal line) are also shown. Deposition is a positive excursion and elution zones are  
 5 negative excursions from the mean in each diagram. A lowpass filter (half-year moving  
 6 average) is shown in red. Different periods of deposition and elution have been noted with  
 7 roman numbers.

Deleted: 8

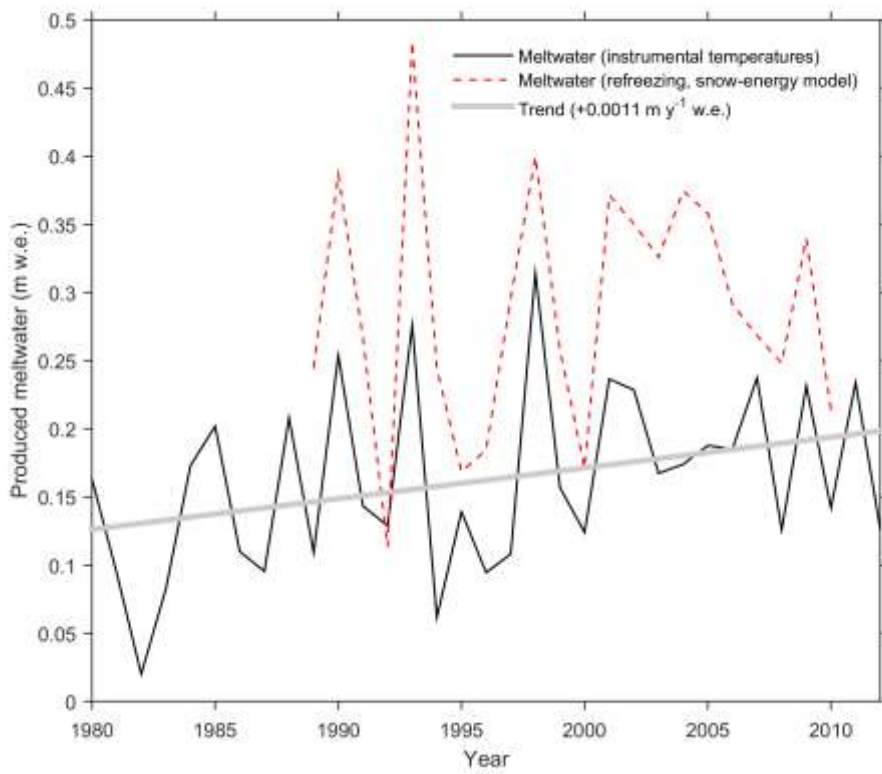
Deleted: dashed black

Deleted: ¶

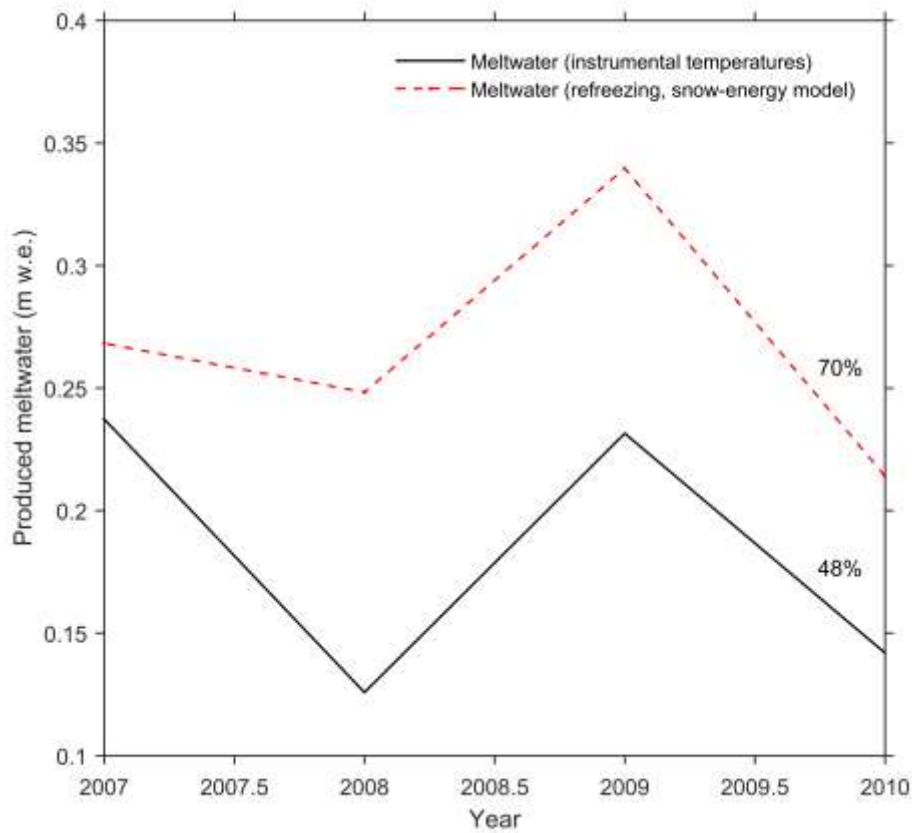


1  
2 Figure 9 Number of ice layers found at different depths in the: LF-97 (left), LF-09 (centre)  
3 and LF-11 (right) ice cores. The ice layers were divided in three classes according to their  
4 thickness: thin layers (\*), medium-thick layers (∇) and thick layers (●).

5

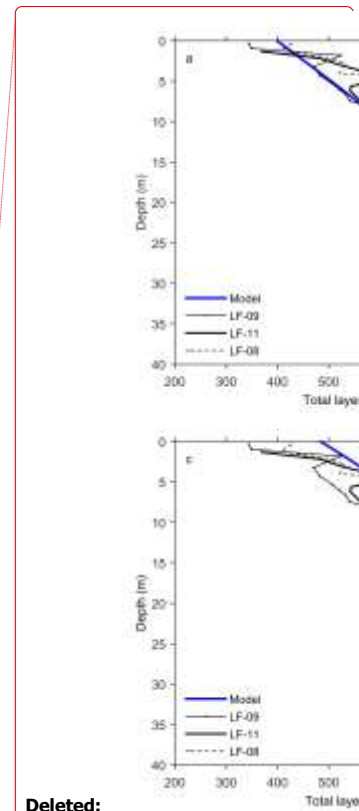
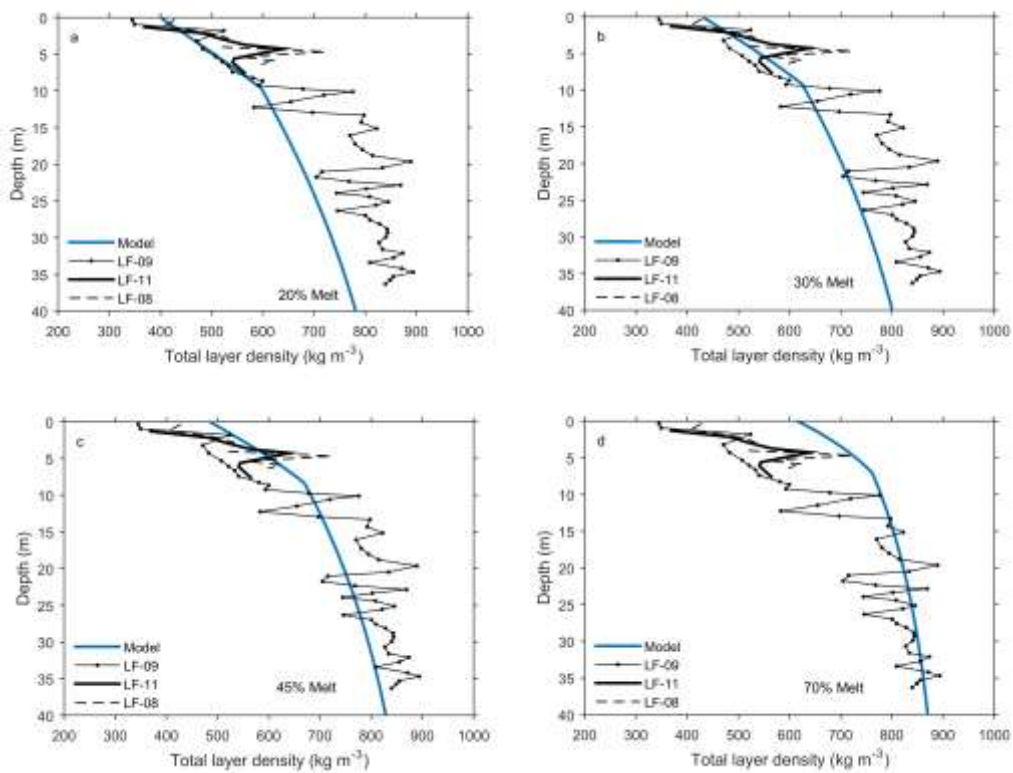


1  
 2 Figure 10 Produced meltwater calculated at Lomonosovfonna using the PDD (black) and  
 3 snow-energy model (dashed red) approaches. The linear trend of meltwater calculated with  
 4 the PDD approach and instrumental temperatures is also shown over the 1979–2012 period  
 5 (grey).  
 6



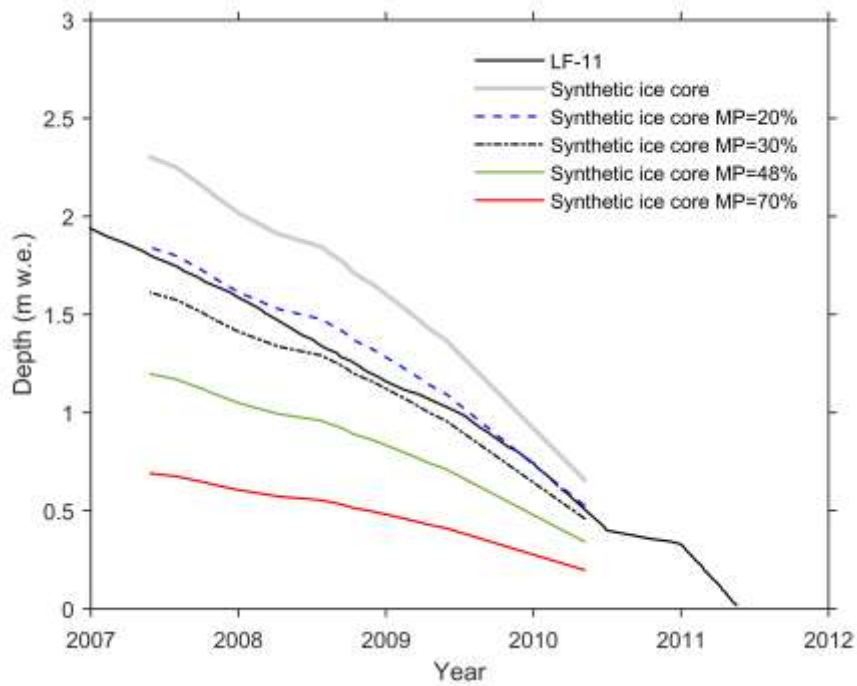
1  
 2 Figure 11 Meltwater calculated at Lomonosovfonna during the period 2007–2010 using the  
 3 different approaches: PDD and instrumental temperatures (black); and the snow-energy model  
 4 (dashed red). The percentages above each line represent the average melt percentage (MP)  
 5 during the studied period, estimated by the different approaches.

6



1  
 2 Figure 12 Comparison between the LF-08, LF-09 and LF-11 ice core density profiles (annual  
 3 averages) and the output of the firn-densification model (*Reeh et al. 2005*), considering: a)  
 4 20% of melt, b) 30% of melt, c) 45% of melt, and d) 70% of melt.

5



1  
 2 Figure 13 Depth–time scales for the LF-11 and LF-syn ice cores during 2007–2011 (black and  
 3 grey lines, respectively). Blue dashed, black-dot-dashed, green and red lines represent the  
 4 synthetic core depth–time scale considering a MP of 20 %, 30 %, 48 % and 70 %, respectively.  
 5  
 6